LUND UNIVERSITY

Adsorption, desorption, and redox reactions at iron oxide nanoparticle surfaces

Krumina, Lelde

2017

Link to publication

Citation for published version (APA):
Krumina, L. (2017). *Adsorption, desorption, and redox reactions at iron oxide nanoparticle surfaces*. [Doctoral Thesis (monograph), Centre for Environmental and Climate Science (CEC), Department of Biology]. Lund University, Faculty of Science, Centre for Environmental and Climate Research (CEC), Department of Biology.

Total number of authors:
1

General rights
Unless other specific re-use rights are stated the following general rights apply:
Copyright and moral rights for the publications made accessible in the public portal are retained by the authors and/or other copyright owners and it is a condition of accessing publications that users recognise and abide by the legal requirements associated with these rights.
• Users may download and print one copy of any publication from the public portal for the purpose of private study or research.
• You may not further distribute the material or use it for any profit-making activity or commercial gain
• You may freely distribute the URL identifying the publication in the public portal

Read more about Creative commons licenses: https://creativecommons.org/licenses/

Take down policy
If you believe that this document breaches copyright please contact us providing details, and we will remove access to the work immediately and investigate your claim.

LUND UNIVERSITY

PO Box 117
221 00 Lund
+46 46-222 00 00

Download date: 04. May. 2026

Adsorption, desorption, and redox reactions at iron oxide nanoparticle surfaces

LELDE KRUMINA
ENVIRONMENTAL SCIENCE | CEC AND DEPARTMENT OF BIOLOGY | LUND UNIVERSITY

Adsorption, desorption, and redox reactions at iron oxide nanoparticle surfaces

Lelde Krumina

LUND
UNIVERSITY

DOCTORAL DISSERTATION
by due permission of the Faculty of Science, Lund University, Sweden.
To be defended at Blue Hall, Ecology Building, Sölvegatan 37, Lund, Sweden on the 25th of January 2018 at 10:00.

Faculty opponent
Dr. Katharina Müller, Helmholtz-Zentrum Dresden-Rossendorf (HZDR), Institute of Resource Ecology, Dresden, Germany

Organization
LUND UNIVERSITY

Centre for Environmental and Climate Research
Sölvegatan 37
SE-226 62 Lund

Author: Lelde Krumina

Document name
DOCTORAL DISSERATION

Date of issue
18/12/2017

Sponsoring organization

Title and subtitle
Adsorption, desorption, and redox reactions at iron oxide nanoparticle surfaces

Abstract:
Iron oxide nanoparticles are involved in several important biogeochemical processes. The interfaces between aqueous solutions and iron oxide nanoparticle surfaces are found everywhere in nature, and the chemical and microbial processes occurring at these complex interfaces control e.g. nutrient and contaminant availability and transport. Recently, it has been shown that certain ectomycorrhizal (ECM) fungi decompose dissolved organic matter (DOM) via non-enzymatic reactions involving the attack by reactive oxygen species (ROS), particularly the hydroxyl radical (•OH) generated via the Fenton reaction ($Fe^{2+} + H_2O_2 \rightarrow Fe^{3+} + {}^{\bullet}OH + OH^-$). Previous studies on fungal non-enzymatic DOM decomposition included soluble Fe^{3+} complexes that were reduced by metabolites to Fe^{2+} in order to initiate the Fenton reaction. However, the mechanisms of •OH formation in soil environments where solid and low-solubility iron oxide nanoparticles are the predominating iron source, are very much unknown.

This thesis focused on the reactions between ferrihydrite or goethite nanoparticles and the model metabolite 2,6-dimethoxyhydroquinone (2,6-DMHQ) or DOM modified by the ECM fungus *P. involutus*. These reactions were studied at different experimental conditions, primarily varying pH and the O_2 level. In order to accomplish the set aims, this PhD project included batch experiments combined with conventional wet-chemical analyses as well as the Simultaneous Infrared and Potentiometric Titration (SIPT) method to monitor the reactions at the water-mineral interfaces in real-time.

The overall results showed that iron oxide nanoparticles were reductively dissolved by 2,6-DMHQ at pH 4.0 and 4.5. Under aerobic conditions these reactions produced both Fenton reagents and •OH was generated. The extent of •OH generation was sensitive to the reduction potential (E_H) of the iron oxide, the O_2 concentration and the competitive adsorption of organic and inorganic anions. The reactions between 2,6-DMHQ and the iron oxides at pH 7.0 and under aerobic conditions generated low amounts of •OH. At these conditions reductive dissolution was of minor importance. Instead, catalytic oxidation of 2,6-DMHQ produced H_2O_2 that partly was degraded by the iron oxide surfaces into •OH. Co-adsorbed anions further promoted this process,

DOM modified by *P. involutus* increased the reductive dissolution of iron oxides at pH 4.0 as compared to fresh DOM. Reactions between the Fe^{2+} produced and H_2O_2 generated •OH that preferentially oxidized some of the DOM components. These results suggested that modified DOM contained secondary metabolites that possibly serve both as iron reducers and antioxidants.

This thesis has provided new knowledge on the complex reaction mechanisms between iron oxide nanoparticles and redox-active organic compounds. It has increased the understanding of non-enzymatic •OH generation, and the knowledge obtained will help to understand the role of this process in organic matter decomposition. Finally, the research has identified possible mechanisms behind toxicity of iron oxide nanoparticles.

Key words: Ferrihydrite, goethite, secondary metabolites, 2,6-DMHQ, reductive dissolution, catalytic oxidation, hydroxyl radicals, Fenton reaction, SOM decompositttion

Classification system and/or index terms (if any)

Supplementary bibliographical information | Language: English

ISSN and key title | ISBN
Print: 978-91-7753-503-4
Pdf: 978-91-7753-504-1

Recipient's notes | Number of pages 216 | Price

Security classification

I, the undersigned, being the copyright owner of the abstract of the above-mentioned dissertation, hereby grant to all reference sources permission to publish and disseminate the abstract of the above-mentioned dissertation.

Signature _____ Date 2017-12-18

Adsorption, desorption, and redox reactions at iron oxide nanoparticle surfaces

Lelde Krumina

LUND
UNIVERSITY

Cover design by Agrita Sile and Lelde Krumina

Bottom photo reprinted by permission of Prof. David J. Read

Copyright Lelde Krumina

Faculty of Science
Centre for Environmental and Climate Research, Department of Biology

ISBN 978-91-7753-503-4 (print)
ISSN 978-91-7753-504-1 (pdf)

Printed in Sweden by Media-Tryck, Lund University
Lund 2017

MADE IN SWEDEN

Media-Tryck is an environmentally certified and ISO 14001 certified provider of printed material. Read more about our environmental work at www.mediatryck.lu.se

Table of Contents

List of papers

I. Krumina, L., Lyngsie, G., Tunlid, A., Persson, P. Oxidation of a dimethoxyhydroquinone by ferrihydrite and goethite nanoparticles: Iron reduction versus surface catalysis. *Environmental Science & Technology*, 51, 9053-9061, 2017.

II. Lyngsie, G., Krumina, L., Tunlid, A., Persson, P. Generation of hydroxyl radicals from reactions between a dimethoxyhydroquinone and iron oxide nanoparticles. *Submitted to Environmental Science: Nano*.

III. Krumina, L., Persson, P. Mutual influence of hydroquinone oxidation and phosphate adsorption at iron oxide surfaces. *Manuscript.*

IV. Krumina, L., Kenney, J. P.L., Loring, J. S., Persson, P. Desorption mechanisms of phosphate from ferrihydrite and goethite surfaces. *Chemical Geology*, 427, 54-64, 2016.

V. Krumina, L., Ob De Beeck, M., Tunlid, A., Persson, P. Fungal decomposition of dissolved organic matter (DOM): Consequences for reductive dissolution of iron oxides and hydroxyl radical production. *Manuscript.*

Papers I and IV are reprinted with permission from the publishers.

The following paper is not included in the thesis.

Arshanitsa, A., Krumina, L., Telysheva, G., Dizhbite, T. Exploring the application potential of incompletely soluble Organosolv lignin as a macromonomer for polyurethane synthesis. *Industrial Crops and Products*, 92, 1-12, 2016.

Author's contributions to the papers

I. LK, GL, AT and PP conceived and designed the experiments. LK performed the experiments. LK and PP did data analysis and wrote the paper with inputs from co-authors.

II. LK, GL, AT and PP conceived and designed the experiments. LK and GL performed the experiments. GL, LK, AT and PP did data analysis and wrote the paper.

III. LK, and PP conceived and designed the experiments. LK performed the experiments. LK, and PP did data analysis and wrote the paper.

IV. LK, PP, JPLK and JSL conceived and design the experiments. LK and JSL performed the IR spectroscopy experiments. LK and PP did data analysis and wrote the paper with inputs from co-authors.

V. LK, AT and PP conceived and designed the experiments. MODB did incubation of *Paxillus involutus* on dissolved organic matter. LK performed the experiments. LK and PP did data analysis and wrote the paper with inputs from co-authors.

LK: Lelde Krumina

PP: Per Persson

AT: Anders Tunlid

GL: Gry Lyngsie

JPLK: Janice P. L. Kenney

JSL: John S. Loring

MODB: Michiel Op De Beeck

Abbreviations and acronyms

•OH	Hydroxyl radical
•OOH	Superoxide
2,5-DMHQ	2,5-dimethoxyhydroquinone
2,6-DMBQ	2,6-dimethoxybenzoquinone
2,6-DMHQ	2,6-dimethoxyhydroquinone
2-MHQ	2-methoxyhydroquinone
AOPs	Advanced oxidation processes
C	Carbon
CO_2	Carbon dioxide
DFT	Density functional theory
DOM	Dissolved organic matter
ECM	Ectomycorrhizal
E_H	Reduction potential
Fe^{2+}	Ferrous iron
Fe^{3+}	Ferric iron
H_2O_2	Hydrogen peroxide
H_2Q	Hydroquinone
HPLC	High performance liquid chromatography
HSQ	Semiquinone
hTPA	Hydroxyl terephthalic acid
IR	Infrared
ISCO	In situ chemical oxidation
MCR-ALS	Multivariate curve resolution– alternating least square

O_2	Oxygen
P_i	Phosphate
Q	Quinone
ROS	Reactive Oxygen Species
SIPT	Simultaneous Infrared and Potentiometric Titration
SOM	Soil Organic Matter
TPA	Terephthalic acid, benzene-1,4-dicarboxylic acid

Popular science summary

Soils play a critical role in the carbon (C) cycle by regulating the atmospheric carbon dioxide (CO_2) levels, and correspondingly the Earth's climate. However, there are still countless questions of how biological and geochemical soil processes affect the C cycle. To be able to predict future implications on the Earth's climate, we need to understand these processes. Globally, soils store more C than the terrestrial biomass and the atmosphere combined. The soil environment has an enormous impact on the soil C dynamics, whether C is captured, stored or released. Thus, depending on the soil environment, some soil organic matter (SOM) can persist for decades, while some SOM decomposes more rapidly. It has been shown that soil microbes (fungi, bacteria, archaea, etc.) play an important role in SOM decomposition into smaller molecules, ultimately, releasing CO_2 to the atmosphere or playing an important role in the formation of soil aggregates, thus contributing to increased SOM stability.

Boreal and temperate forests store a large part of the terrestrial C, and in this environment ectomycorrhizal (ECM) fungi are abundant. ECM fungi form symbiotic relationships with plants i.e., plant hosts provide C as energy source for fungal growth and in return fungi transport nutrients to the plant host. A major part of soil nutrients is found in organic form, as part of SOM. Thus, to access and mobilize these nutrients, fungi are required to decompose SOM. Some ECM fungi use a degradation mechanism involving the Fenton reaction ($Fe^{2+} + H_2O_2 \rightarrow Fe^{3+} + {\bullet}OH + OH^-$). For this mechanism to occur, the fungi need ferrous iron (Fe^{2+}) and hydrogen peroxide (H_2O_2). H_2O_2 can be provided by fungi, however, in soils iron is primary found in oxidation state +3 and in solid state as iron oxides and other iron-containing minerals, and thereby, is not easily available. During the initial SOM decomposition, fungi produce low molecular weight organic compounds, secondary metabolites, which are not involved in sustaining fungi or the plant host growth. Some of these secondary metabolites have iron reducing capacity, which can reduce soluble ferric iron (Fe^{+3}) salts, thus making Fe^{2+} more accessible. However, there is limited knowledge on how these secondary metabolites interact with and possibly reduce solid iron oxides.

In this thesis, common boreal and temperate forest soil iron oxides, ferrihydrite and goethite, were used to investigate whether Fenton reactions can be initiated by organic reductants, similar to fungal secondary metabolites or as part of dissolved organic matter (DOM), under different geochemical conditions. The aims of this

PhD project were achieved by studying adsorption, desorption, and redox reactions between the iron oxide nanoparticles and these organic reductants. This research seeks to answer the question of whether some of these reactions can promote the generation of hydroxyl radicals (•OH) via Fenton reaction. Increased understanding of these mechanisms can improve our understanding of the stability of SOM and SOM-mineral aggregates.

Results obtained at pH 4.5 and 4.0 showed that a model compound (2,6-DMHQ), which is similar to a compound secreted by brown rot wood decay fungi, was able to reductively dissolve iron oxide nanoparticles and produce H_2O_2 under aerobic reaction conditions. Thus, reactions between 2,6-DMHQ and iron oxides allow the formation of both reactants to initiate the Fenton reaction. In anaerobic environments, due to a lack of oxygen (O_2), the formation of H_2O_2 was negligible from reactions between 2,6-DMHQ and iron oxides, thus suppressing the Fenton reaction. Moreover, results showed that initiation of the Fenton reaction was not only affected by O_2 concentrations, but also by different geochemical factors, such as pH, redox potentials and adsorption of organic and inorganic molecules.

Soils contain a wide range of inorganic and organic molecules that can adsorb on iron oxides, thus interfering with redox reactions at iron oxide surfaces. Results showed that 2,6-DMHQ was able to compete with inorganic and organic molecules for surface iron and to initiate the Fenton reaction. Moreover, adsorption of organic and inorganic molecules in some cases promoted the Fenton reaction to occur close to iron oxide nanoparticle surfaces. These surface reactions can have a considerable impact on adsorbed SOM decomposition and the provision of nutrients to plant hosts. At the same time, more extensive SOM decomposition can result in a greater CO_2 release.

At neutral pH values, various organic pollutants, with molecular structures similar to 2,6-DMHQ, are found in groundwater and agricultural soils due to pesticide and fertilizer use. Injection of H_2O_2 into the soil or aquatic systems is a widely-applied technique to degrade these pollutants. Results at pH 7.0 showed that adsorption of inorganic and organic molecules on iron oxides resulted in a higher yield of the Fenton reaction from the 2,6-DMHQ-iron oxide interactions. Therefore, naturally occurring processes between iron oxides and 2,6-DMHQ-like molecules can help to increase organic contaminant degradation, for example, when the commonly added plant nutrient, phosphate, is adsorbed on iron oxide surfaces.

DOM modified by the ECM fungus *Paxillus involutus*, which contained secondary metabolites, has a higher affinity towards iron oxide surfaces than the initial DOM. This is in agreement with the hypothesis that organic matter decomposition can contribute to SOM stability. Results showed that modified DOM reductively dissolved ferrihydrite and goethite, but in order to initiate the Fenton reaction the addition of H_2O_2 was required. Further, results suggested that in the absence of

H_2O_2, some Fe^{2+} was complexed to adsorbed DOM. When H_2O_2 was added the Fenton reaction occurred in close vicinity to the organic matter, which resulted in direct oxidation of DOM components. Moreover, experiments with DOM modified by *P. involutus* suggested that the produced secondary metabolites might act as antioxidants. Thus, these metabolites may inhibit the oxidation of other DOM components, thereby increasing the partial recalcitrance of DOM.

In summary, the results obtained in this PhD project suggested that in aerobic soil environments and in the presence of iron oxide nanoparticles, fungal secondary metabolites with molecule structures similar to 2,6-DMHQ might initiate the Fenton reaction and produce •OH. Yet, further studies are required to understand if and how these reactions affects the stability of the soil C. Moreover, the generation of •OH at iron oxide nanoparticles surfaces can be harmful and cause damage to organisms exposed to these nanoparticles. Thus, the reactions characterized in this study can be related to the potential toxicity of iron oxide nanoparticles.

Introduction

Nanoparticles have always been present in the Earth's systems because of various weathering and precipitation processes. Thus, life has evolved in the presence of nanomaterials, and consequently we are already aware of some of their broader implications for living organisms and ecosystems.[1,2] Iron is the fourth most common element and different iron oxide nanoparticles are widely distributed in the Earth's crust. In addition, diverse iron oxide nanoparticle properties are studied and applied in fields, such as in biomedicine,[3–12] groundwater and wastewater treatment,[13–18] and other fields of application.[19–25] Accordingly, today the importance of environmental nanoparticles is unquestionable and highly recognized.

A challenge in geochemical research is to understand the roles that nanoparticles play in the distribution and bioavailability of elements, mineral growth and dissolution, and in catalysis and reaction pathways. In soils, iron oxide nanoparticles and other iron-containing minerals play an important role in numerous geochemical processes. Many studies have focused on adsorption/desorption processes[26–31] and redox reactions,[32–40] where iron oxides have been shown to be strong adsorbents and catalysts. In general, the results from those studies were attributed to properties of the iron oxides, such as surface area, particle size, morphology, surface chemistry and that iron oxide reactivity increases with increasing surface area. However, adsorption/desorption and redox reactions in the soil environment can also be influenced by other factors, such as pH, reduction potential (E_H), O_2 concentration, adsorption of competing molecules, microorganism diversity, aeration, temperature, etc.[41,42]

Increasing attention is on SOM adsorption on minerals because SOM stores large fractions of terrestrial C,[43,44] and the stability of SOM has been shown to be associated with SOM adsorption onto secondary aluminum and iron minerals.[45–47] In addition to mineral adsorption effects, SOM stability is also influenced by interactions between SOM and other components of the biological, physical and chemical environments. Soil microbes decompose SOM to access nutrients, yet organic matter can be inaccessible for microbes due to incorporation into micro-pores and aggregates. These aggregates can be stabilized by hydrophobic interactions and hydrogen bonding forces.[44,48,49] Although various protective mechanisms have been proposed to explain SOM stability, contributions of these factors are still not completely understood. In general, two SOM decomposition

pathways by microbes have been recognized: (1) the enzymatic decomposition pathway, which depends on extracellular enzymes, and (2) the non-enzymatic decomposition pathway, which involves reactive oxygen species (ROS), particularly •OH generated via the Fenton reaction. The Fenton reaction requires mechanisms for iron reduction, which may be accomplished by extracellular metabolites, cellobiose dehydrogenases or redox-active peptides.[50–52] Wood decay studies have shown that brown-rot fungi are able to degrade wood polymers through a combination of non-enzymatic and enzymatic mechanisms. In one of these processes, brown-rot fungi produce the secondary metabolite 2,5-dimethoxyhydroquinone (2,5-DMHQ) which is able to reduce iron and form H_2O_2 in aerobic environments, thus producing both Fenton reactants.[53–57] These results propose hydroquinones to be favourable organic substance to initiate •OH generation. Hydroquinone and hydroquinone-like molecules have been acknowledged as important redox-active components in soil and aquatic organic matter,[58] and due to their redox properties they are used in agro- and industrial products. Moreover, because of resonance-stabilization of intermediate semiquinone (HSQ), hydroquinones are recognized as important electron transfer mediators in several biogeochemical processes, such as organic pollutant degradation and iron bioreduction.[59]

Studies on wood decay by brown-rot fungi and SOM decomposition caused by the ECM fungus *P. involutus* have shown that these fungi use Fenton reaction mechanisms in the presence of soluble Fe^{3+} salts. Yet, it is unknown if and how these mechanisms operate in a soil environment where iron oxides of low solubility predominate. Hence, there is a gap in knowledge on whether soil fungal secondary metabolites can reductively dissolve iron oxides and/or other iron-containing minerals and concomitantly generate favourable conditions for the Fenton reaction. This PhD project was focused on improving our current understanding of these reactions by studying adsorption, desorption and redox processes involving ferrihydrite and goethite nanoparticles and the model compound 2,6-DMHQ and DOM modified by *P. involutus*. This was accomplished by combining wet chemical analysis with *in-situ* infrared (IR) spectroscopy to study reactions at water-nanoparticles interfaces in laboratory experiments.

Background

Iron oxides and their role in biogeochemical processes

The role and effects of iron oxides in biogeochemical processes are widely studied due to their common occurrence in natural systems.[60] In soils, the composition and crystallinity of the iron oxides are controlled by precipitation and dissolution reactions that depend on several factors, such as pH, temperature and redox conditions.[60] Due to their thermodynamic stability, goethite and hematite are two of the most common iron oxides in soils and sediments. Goethite has been found in most soil types, while hematite mostly occurs in tropical and subtropical soil areas.[60] In nature, formation of both oxides is instigated by the slow transformation of thermodynamically unstable ferrihydrite through dissolution and re-precipitation reactions. Formation of ferrihydrite occurs via rapid Fe^{3+} hydrolysis and is characterized as a poorly crystalline iron oxide, usually in the form of nano-sized spherical particles with a large surface area.[60,61]

Iron oxides, in soils and sediments, are strong sorbents and are involved in numerous environmental processes, such as regulating the availability of plant nutrients (Figure 1).[62] Plants and microbes need iron as a nutrient, but since iron occurs mainly in the solid state as Fe^{3+}, plants and microbes have evolved several iron uptake mechanisms that involve dissolution and complexation by small organic acids and molecules with high iron affinity, sometimes also involving iron reduction by redox-active compounds.[63,64] Common electron donors and iron reducing compounds in soil environments are the hydroquinone- and phenol-like molecules.[39,59,65,66] It has been shown that these compounds can be produced by different organisms, such as microbes and insects, and they are also believed to be a part of SOM.[59,67,68]

In wastewater and groundwater treatment, iron oxides and other iron-containing minerals are applied as sorbents for heavy metal adsorption and/or as catalysts in organic contaminant degradation. Since heavy metals in drinking water are toxic for humans, numerous studies have been devoted to adsorption of arsenic (As)[69–71] and other heavy metals.[16] Iron-containing minerals are also used as catalysts in organic pollution degradation by exploiting Fenton chemistry reactions.[33,72]

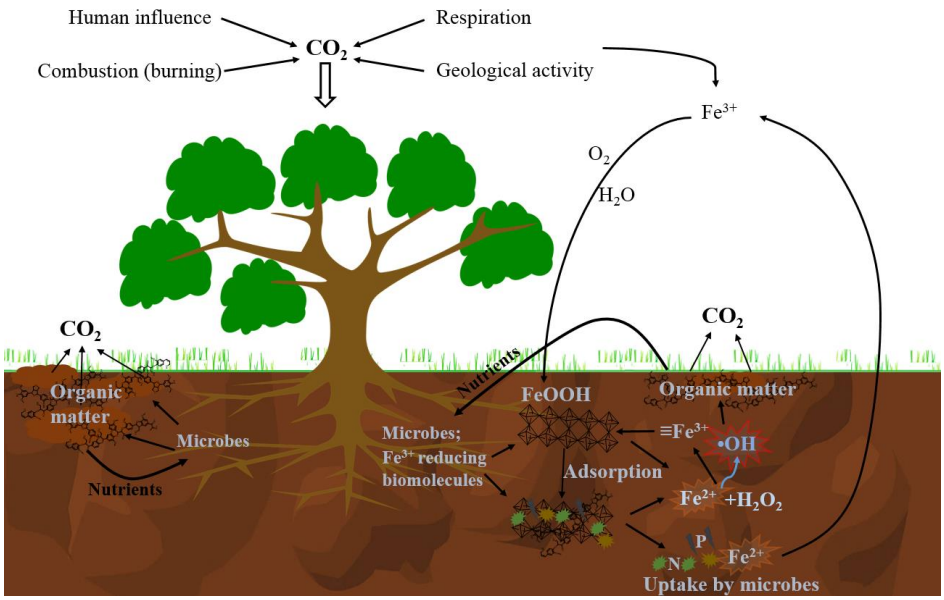

Figure 1. Iron and carbon interactions in biogeochemical cycles

Soil organic matter decomposition by fungi

Soils are the largest C sink, but it is still unclear why some SOM persists for decades, while other SOM is decomposed more rapidly. In general, decomposition of SOM is controlled by soil microbial activity and the complex physical and chemical interactions in soils.[44,73–75] Previous studies on SOM decomposition by microbes have focused mostly on the role of enzymes, and it has been shown that fungi and bacteria use a large variety of enzymes in these processes. In addition, recent data suggest that certain ECM fungi may use non-enzymatic mechanisms to decompose SOM (Figure 2). These processes involve the attack by ROS, including the short-lived and non-selective •OH generated through the Fenton (R1), the Fenton-like (R2) or the Haber-Weiss reactions (R3).[76] Further in the text reactions R1-3 are denoted as Fenton reactions.

$$Fe^{2+} + H_2O_2 \rightarrow Fe^{3+} + \bullet OH + OH^- \qquad (R1)$$

$$Fe^{3+} + H_2O_2 \rightarrow FeOOH^{2+} + H^+ \qquad (R2)$$

$$FeOOH^{2+} \rightarrow Fe^{2+} + \bullet OOH$$

$$Fe^{2+} + H_2O_2 \rightarrow Fe^{3+} + \bullet OH + OH^-$$

$$Fe^{3+} + O_2^{\bullet-} \rightarrow Fe^{2+} + O_2 \qquad (R3)$$

$$Fe^{2+} + H_2O_2 \rightarrow Fe^{3+} + \bullet OH + OH^-$$

These reactions require Fe^{2+}, which is not thermodynamically stable in aerobic soils and is rapidly oxidized to Fe^{3+} that subsequently is precipitated as iron oxides or strongly complexed by organic ligands making it less available for the Fenton reactions.[77,78] Three iron reduction mechanisms have been proposed to initiate ROS-based organic matter decomposition: (1) iron-reducing enzymes (ferric reductases, cellobiose oxidases, cellobiose dehydrogenases,[52] (2) low-molecular weight glycopeptides,[50] and (3) low-molecular weight redox active aromatic molecules (quinones).[51]

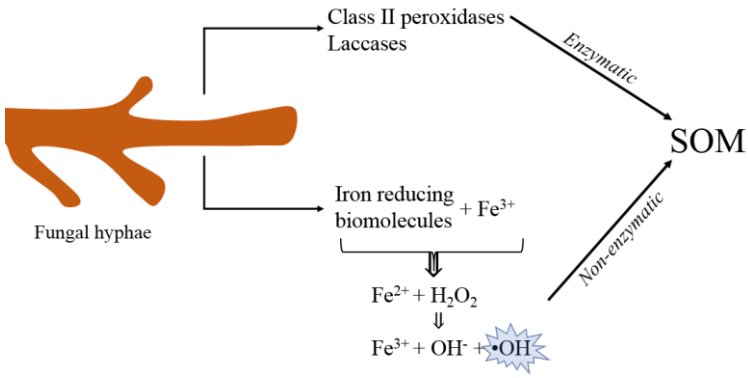

Figure 2. Fungal SOM decomposition by enzymatic and non-enzymatic reactions.

The secondary metabolite involutin (diarylcyclopentenone), produced by the ECM fungus *P. involutus* has been found to be involved in iron reduction.[79] Involutin is therefore an important part of the machinery generated by *P.involutus* to decompose SOM via the Fenton reaction. However, in this process it is still unknown how H_2O_2 is produced, even though the genome of *P. involutus* encodes a number of genes for H_2O_2 production that could be involved in this process.[76]

Wood decay studies on brown-rot fungi have identified the secondary metabolite 2,5-DMHQ as an Fe^{3+} reducing compound, which can initiate the Fenton reaction under aerobic reaction conditions (Figure 3); i.e. it has the capacity to produce Fe^{2+} and H_2O_2 via reduction of Fe^{3+} and O_2. This secondary metabolite has been identified in three distantly related brown-rot fungal species,[53–57,80] suggesting that the biosynthetic pathway for 2,5-DMHQ existed in a common ancestor and 2,5-DMHQ might therefore be a rather widespread secondary metabolite. Secondary metabolites, similar to 2,5-DMHQ, have not been identified in cultures of *P. involutus* or other ECM fungi. However, hydroquinone and hydroquinone-like

molecules are formed naturally,[59] thus hydroquinone and hydroquinone-like molecules could contribute to iron reduction and bioavailability.

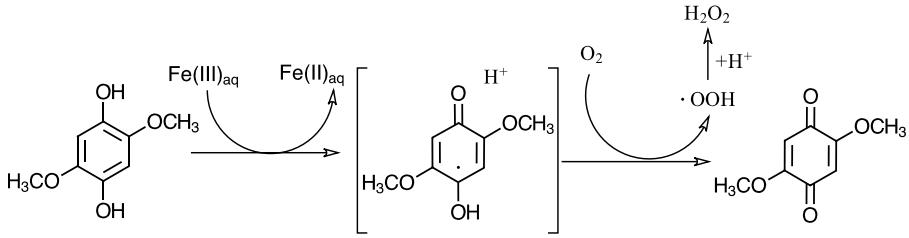

Figure 3. Proposed reaction pathway for Fe^{3+} reduction and H_2O_2 production from wood decay studies via oxidaion of 2,5-DMHQ.[56]

Studies on *P. involutus* and brown-rot wood-decayers have used soluble Fe^{3+} salts, while in the soil, iron generally is found in a solid state as iron oxides and/or other iron-containing minerals. In the soil, iron oxides precipitate and form more crystalline iron oxide nanoparticles with increasing soil depth, which become thermodynamically more stable with increasing aging time. For certain ECM fungi, or other microbial species, to initiate •OH generation in the soil environment, reduction of iron oxides is required. Thus, it is unclear if the secondary metabolites of *P.* involutus and hydroquinone-like molecules could initiate Fenton reactions in the presence of iron oxides and/or iron-containing minerals.

Reactions between hydroquinones and iron oxides

The well-studied redox triad quinone/semiquinone/hydroquinione (Q/HSQ/H_2Q), coupled via 1 electron transfer reactions, makes quinones effective electron shuttles in biological systems and contaminant degradation.[59,81] Hydroquinone oxidation is characterized through three reaction pathways:[81]

(1) Hydroquinone autoxidation in the presence of O_2;

$$H_2Q + O_2 \rightarrow Q + H_2O_2 \qquad (R4)$$

(2) Catalytic oxidation by redox metals as catalysts in the presence of O_2;

$$H_2Q + O_2 \xrightarrow[catalyst]{FeOOH} Q + H_2O_2 \qquad (R5)$$

(3) Hydroquinone oxidation through metal ($\equiv Fe^{3+}$) reductive dissolution;

$$H_2Q + 2FeOOH \rightarrow Q + 2Fe^{2+} + 4OH^- \qquad (R6)$$

Simple hydroquinone and hydroquinone-like molecules have been studied with respect to their capability of iron oxide reduction, and also in relation to organic pollutant oxidation. Several of these studies involved 1,4-hydroquinone and catechol (1,2-dihydroxybenzene) and were performed under anaerobic conditions, thus excluding reactions R4 and R5.[34,37,39,82,83] In general, the reaction stoichiometry was reported to be 1 H_2Q: 2 Fe^{2+}: 1 Q and the iron oxide reactivity towards hydroquinone oxidation increased with increasing specific surface area and decreasing particle size. Studies under aerobic reaction conditions have used iron-containing materials as catalysts for hydroquinone- and phenol-like oxidation.[65,84–87] While no H_2Q: Fe ratios were reported, results suggested there was formation of new oxidation products. Polymer-like products indicated reactions between intermediate semiquinone radicals.[65,86] Other studies reported ring cleavage products, and the formation of aldehydes,[88] carboxylic acids and ethers.[89] Moreover, in the presence of amorphous iron oxides, oxidation of the plant secondary metabolite catechin resulted in both polymerization and CO_2 formation.[87] The aliphatic products were proposed to be formed via •OH attack on aromatic rings by H abstraction and addition to unsaturated C-C bonds.[90]

Putting these results into perspective of SOM decomposition, these previous results have shown that hydroquinone and hydroquinone-like molecules were able to reductively dissolve iron oxide particles and likely also generate •OH via the Fenton reaction. At the same time, in the presence of O_2 different types of side-products were formed from the oxidation of hydroquinones. This would mean that with each redox cycle, there will be a loss of quinones and less molecules available for enzymatic regeneration of the hydroquinone.[81] Hence, to maintain the Fenton reactions, fungi would be required to continuously produce secondary metabolites or control the conditions to maintain the formation of side-products at a low level.

Reactions between hydrogen peroxide and iron oxides

Hydroquinone and hydroquinone-like molecules have been shown to produce both Fenton reaction components (i.e., Fe^{2+} and H_2O_2) from a soluble Fe^{3+} source. However, as stated above, iron exist as iron oxides and other iron-containing minerals in soil environments, and as soon surfaces are involved, the generation of •OH become more complex.[91,92] Recently, it has been proposed that iron oxide nanoparticles can initiate •OH generation via five different pathways (Figure 4).[93]

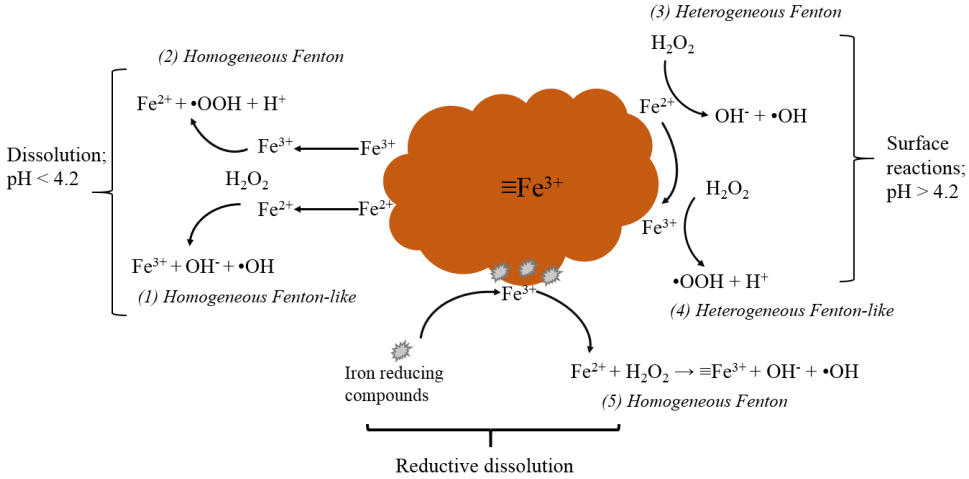

Figure 4. Proposed reactions of •OH generation by iron oxide nanoparticles[93]

While heterogeneous Fenton reactions are not well understood, these systems have shown several differences with respect to homogeneous Fenton reactions. Homogeneous Fenton reactions have the highest efficiency at ca. pH 3.0 and the oxidized Fe^{3+} is often precipitating. In contrast, iron oxides and iron-containing materials are decomposing H_2O_2 via surface bound iron, thus avoiding iron precipitation and operate over a wider pH range.[94,95]

Iron oxide or iron-containing mineral surfaces can decompose H_2O_2 through two reaction pathways: (1) formation of O_2 and H_2O or (2) formation of •OH.[96] H_2O_2 decomposition into O_2 and H_2O has been recognized as an advantage in anaerobic soils where O_2 is introduced into the environment for microbe-initiated bioremediation.[97] H_2O_2 decomposition into •OH are exploited in wastewater treatment methods, such as In Situ Chemical Oxidation (ISCO) and Advanced Oxidation Processes (AOPs) for soil and groundwater organic contaminant mitigation.[98] In these methods, H_2O_2 is injected into the environment containing iron materials to trigger •OH formation via surface initiated chain reactions.[92,96,99,100] Overall, heterogeneous Fenton reactions result in low generation of ROS,[99,101] compared to homogeneous Fenton reactions, where soluble iron is directly available. However, a higher production of H_2O_2 decomposition into •OH, especially at neutral pH values, has been achieved in the presence of adsorbed oxyanions and low molecular weight organic acids.[102–107] Several explanations to these results have been proposed. In addition to chelating and scavenging effects, it has been suggested that ligand adsorption blocked H_2O_2 reactions with surface active sites, thus suppressing iron oxides to act as catalyst for H_2O_2

disproportionation into O_2 and H_2O.[99,105,108] Yet direct experimental confirmation is missing and there is much more challenging research ahead to understand ROS generation mechanisms in the presence of surfaces and adsorbed organic and inorganic molecules.

Impact of adsorbed molecules on redox reactions

In soil environments, iron oxides act as strong adsorbents for different organic and inorganic molecules. Phosphate, due to its strong affinity for iron oxide and iron-containing mineral surfaces, often is a limiting nutrient in soils.[109] Therefore, phosphate desorption is required for phosphate acquisition in acidic environments (pH 3-5). Several desorption mechanisms have been proposed. These are ligand exchange, phosphate release caused by iron oxide dissolution, and iron oxide reductive dissolution by different reducing agents.[110–112] Some studies have indeed showed that phosphate is released via iron oxide dissolution and/or reductive dissolution.[113–115] This implies that redox active secondary metabolites could make phosphate available for microbial and plant uptake.

Most previous laboratory studies have used different buffers, such as phosphate or acetate, to study reactions between hydroquinone/hydroquinone-like molecules and iron oxides. Often the effect of buffer molecules have not been discussed or have been considered to be negligible.[116] Still, there is evidence that nanoparticle catalytic properties can be altered by the presence of a ligand, such as phosphate, adsorption.[117,118] Furthermore, laboratory studies have shown that adsorption of different molecules can decrease reductive dissolution of minerals.[119,120] Thus, adsorption of different molecules could suppress the formation of Fe^{2+}, which correspondingly should result in a lower yield of •OH. On the other hand, other studies on oxidation of organic pollutants have shown that co-adsorbed molecules can increase the formation of •OH.[92] Evidently the impact of adsorbed molecules on Fenton-based •OH generation at mineral surfaces is far from understood.

Aims and objectives

ECM fungi are abundant in boreal and temperate forest soils.[121] The ECM fungus *P. involutus* has been used in the current work as a model ECM fungal species, and previous studies have identified that the secondary metabolite involutin is produced by *P. involutus* and that this molecule is involved in Fenton-based SOM decomposition.[76,79] Furthermore, wood decay studies have shown that three distantly related brown-rot fungal species produce the same secondary metabolite 2,5-DMHQ that has the capability to reduce soluble Fe^{3+} salts and form H_2O_2.[53–55] Based on this knowledge, an overall aim of this thesis was to gain detailed molecular-scale information of the iron oxide nanoparticle interactions with a stable isomer of the 2,5-DMHQ, namely 2,6-dimethoxy-1,4-hydroquinone (2,6-DMHQ), and also with DOM modified by *P. involutus*. Other aims were to investigate how different geochemical factors, such as pH and adsorption of different competing molecules affect the 2,6-DMHQ interactions with iron oxide nanoparticles. To accomplish this, following objectives were formulated.

1. To study how the oxidation pathways of the model compound 2,6-DMHQ, are influenced by surface and bulk reactions in the presence of iron oxide nanoparticles with different crystallinities (**Paper I**);
2. To determine if the model compound 2,6-DMHQ can reductively dissolve iron oxide nanoparticles (**Paper I**) and initiate the generation of •OH (**Paper II**);
3. To determine how adsorption of organic and inorganic molecules (**Paper II & III**) and iron oxide surface properties (**Paper IV**) influenced the reactions in points 1 and 2;
4. To study, if DOM modified by *P. involutus* is capable of reductively dissolving iron oxide nanoparticles and how generation of •OH impacts (adsorbed) DOM (**Paper V**).

Materials and methods

This chapter provides a short overview of the materials and methods used to achieve the set aims and objectives on understanding the iron oxide interactions with the model compound 2,6-DMHQ and the different modifications of DOM. 6-line ferrihydrite nanoparticles were synthesized according to Schwertmann.[61] Ferrihydrite was characterized as amorphous spherical particles with an average diameter of 4-5 nm and with an average surface area of 300 m^2/g (Figure 5, right). Goethite was made following the protocol of Hiemstra and van Riemsdijk.[122] Goethite was characterized as needle-like particles and with an average surface area of 70-90 m^2/g, which was determined by the Brunauer-Emmett-Teller (BET) method (Figure 5, left).[123]

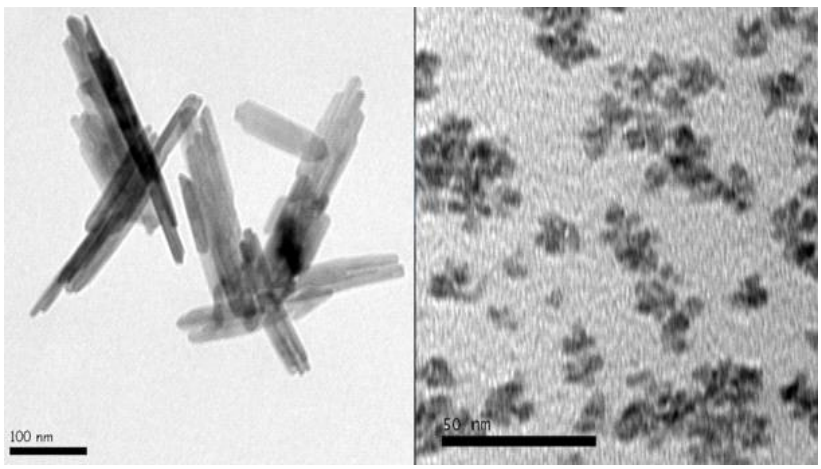

Figure 5. Transmission electron microscopy (TEM) images of goethite (left) and ferrihydrite (right).

All experiments were performed at room temperature (21-23 °C) and solutions were prepared in milli-Q water (18.2 MΩ cm) that was boiled and degassed with N_2 to remove CO_2 from solutions. The test tubes were protected by aluminum foil to avoid exposure to light. In **Papers I-III**, 2,6-DMHQ and in **Paper V**, DOM solutions were prepared fresh before each experiment. Figure 6 summarizes the batch experimental technique applied in this PhD project.

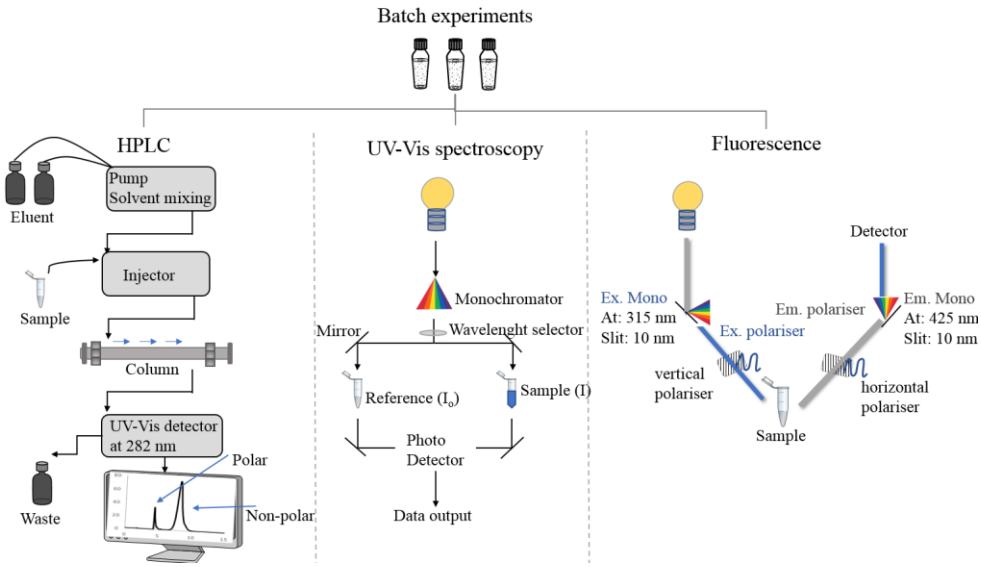

Figure 6. General principles of the batch experimental techniques.

2,6-DMHQ oxidation

High performance liquid chromatography (HPLC) has often been used in environmental monitoring, such as detection of phenolic compounds. Reverse phase HPLC is based on compound polarity separation where the stationary phase is usually nonpolar, but the mobile phase (eluent) is a polar liquid (e.g. a mixture of water and formic acid or acetonitrile). Thus, compounds with high polarity will have shorter retention time, whereas non-polar compounds will take longer time to elute.[124] Reverse phase HPLC chromatography was applied (**Paper I-III**) in order to follow the oxidation of 2,6-DMHQ in the presence of ferrihydrite and goethite under aerobic and anaerobic reaction conditions. These results provided information about 2,6-DMHQ oxidation pathways i.e. catalytic oxidation (R5) and reductive dissolution (R6) reactions. In addition to determination of the 2,6-DMHQ/2,6-DMBQ redox couple, HPLC could detect the intermediate semiquinone radical and oxidation side-products.

Fe^{2+} and phosphate measurements

Colorimetric analysis is based on a color intensity change that depends on concentration of the species of interest, which quantitatively can be measured by

spectrophotometry. The concentration is calculated by applying the Beer-Lambert law, i.e., the linear relationship between absorbance and concentration of absorbing molecular species, and the type and thickness of material the light passes through. Colorimetric assays were applied in quantitative Fe^{2+} and phosphate (P_i) measurements. Fe^{2+} and ferrozine (monosodium salt hydrate of 3-(2-pyri-dyl)-5,6-diphenyl-1,2,4-triazine-p,p'-disulfonic acid) forms a stable purple color complex with maximum absorbance at 562 nm,[125] and phosphate reacted with a molybdenum reagent forms a blue color complex at 885 nm.[126] Fe^{2+} and phosphate data supplemented 2,6-DMHQ results and helped explain interactions between 2,6-DMHQ and the iron oxide nanoparticles.

Quantitative detection of •OH

Over decades several techniques has evolved to improve detection of short-lived •OH.[127] Electron paramagnetic resonance spectroscopy coupled with spin trapping offers the possibility to detect •OH directly, however this technique requires expensive equipment and careful data handling to avoid artifact signals. •OH can also be measured by molecular probes that form stable •OH-derived products and are sensitive enough to be detected at low •OH levels.[127] During the past decade, several fluorescence-based probes have shown to be efficient in quantitative detection of •OH. Terephthalic acid (TPA) is one of those probes and by reactions with short-lived •OH it forms a single fluorescent hydroxyl-TPA (hTPA) product.[128,129] In this thesis, the TPA probe was used to detect •OH generated at iron oxide surfaces and in bulk solutions. One experimental problem was when the surfaces were oversaturated with pre-adsorbed phosphate ligands, then surface TPA was out-competed, and reacted only with •OH formed in solution. Therefore, only a fraction of •OH were likely detected with this experimental setup (**Paper III**).

IR spectroscopy

Simultaneous Infrared and Potentiometric Titration (SIPT) is a powerful method to study reactions at water-mineral interfaces *in-situ* at geochemically relevant ligand concentrations (micro- to nano-molar).[28] The general setup for SIPT is shown in Figure 7 and more detailed principles of SIPT are described in **Paper IV**. IR spectra collected with this method were analyzed by means of a multivariate curve resolution with alternating least squares (MCR-ALS) Matlab script[130,131] and in some case the results were compared to density functional theory (DFT) calculations. MCR-ALS results distinguish adsorbed surface species, which were

characterized by unique IR spectra and provided kinetic concentration profiles of the corresponding species. DFT calculations were used as a support in structural assignment of adsorbed molecules.

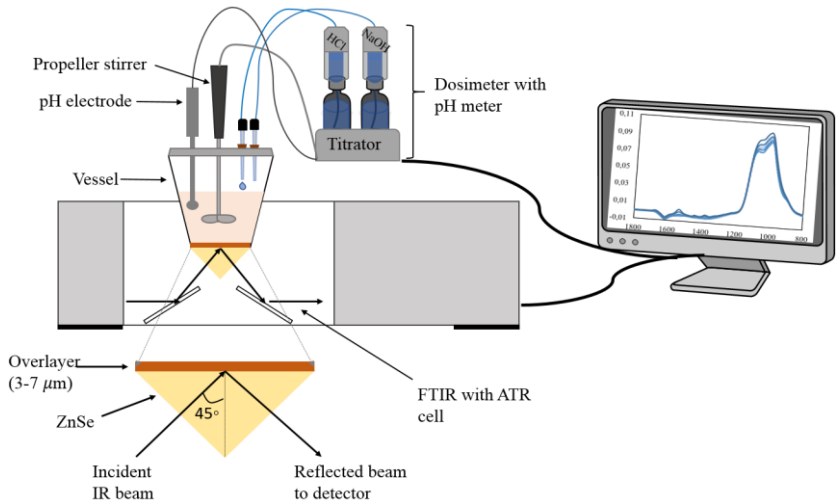

Figure 7. Simultaneous Infrared and Potentiometric Titration setup.

Summary of thesis

The results from this PhD project are summarized in five papers and are discussed in the following chapter. In short, the results showed that 2,6-DMHQ is capable of reductively dissolving iron oxides of different crystallinity (**Paper I**) and under aerobic reaction conditions this process will trigger the Fenton reaction (**Paper II & III**). Adsorption of organic and inorganic molecules changed the surface properties of the iron oxides, and the effects from competing molecules on the reactions between iron oxides and 2,6-DMHQ, and the Fenton reaction were also explored (**Papers II-IV**). Finally, the ECM fungus *P. involutus* was shown to produce iron reducing compounds during DOM decomposition that were capable of reductively dissolving iron oxide nanoparticles. The produced Fe^{2+} was reactive towards added H_2O_2 and the •OH formed via the Fenton reaction resulted in oxidation of DOM (**Paper V**).

2,6-DMHQ oxidation pathways

Comparison between 2,6-DMHQ oxidation in the presence of iron oxides at pH 4.5 and under anaerobic and aerobic reaction conditions helped to distinguish the catalytic oxidation (R5) and reductive dissolution (R6) oxidation pathways **(Paper I)**. At pH 4.5 and under anaerobic conditions after 4 h of the reaction time, 80% and 20% of 2,6-DMHQ was oxidized by ferrihydrite and goethite, respectively, while both minerals oxidized 2,6-DMHQ rapidly in the presence of O_2. These results showed that ferrihydrite could promote both catalytic oxidation (R5) and reductive dissolution (R6), whereas goethite mainly promoted oxidation via a catalytic reaction (R5). It was also shown that at pH 4.5, the anaerobic first order rate constants of 2,6-DMHQ oxidation decreased by close to an order of magnitude. At pH 7.0 and under anaerobic conditions, minor oxidation of 2,6-DMHQ was observed in the presence of both iron oxide nanoparticles. However, under aerobic conditions, 2,6-DMHQ was oxidized rapidly via catalytic oxidation (R5). These results highlighted the important role of O_2 in iron oxide mediated 2,6-DMHQ oxidation. In contrast, Yuan *et al.*[132] proposed that the rapid 2-methoxyhydroquinone (2-MHQ) oxidation in the presence of nanomolar Fe^{3+} was not influenced by O_2 presence because the rate constants of oxidation under aerobic

and anaerobic reactions conditions were similar. Instead, it was proposed that O_2 was involved in oxidizing Fe^{2+} (R7) and/or the HSQ (R8), and the superoxide (•OOH) formation was responsible for the 2-MHQ oxidation.

$$Fe^{2+} + O_2 + H^+ \rightarrow Fe^{3+} + \bullet OOH \quad (R7)$$

$$HSQ + O_2 \rightarrow Q + \bullet OOH \quad (R8)$$

This proposes that mechanism depends on an initial Fe^{3+} reduction by the 2-MHQ (R9).

$$H_2Q + Fe^{3+} \rightarrow HSQ + Fe^{2+} \quad (R9)$$

Hence, the mechanism proposed by Yuan *et al*. requires the formation of Fe^{2+} and the semiquinone through Fe^{3+} reduction, which was occurring only at a slow rate in the presence of iron oxides under our anaerobic conditions at pH 7.0. This implies that Fe^{3+} reduction would be the rate-limiting step also under aerobic conditions if oxidation is driven by the •OOH, and therefore cannot explain the very rapid reaction at pH 7.0 in the presence of both iron oxides **(Paper I)**. Thus, comparison between the homogeneous solutions studied by Yuan *et al*. and our surface reactions emphasized the importance of heterogeneous catalytic oxidation (R5) in the presence of iron oxide surfaces.

2,6-DMHQ reaction mechanisms with ferrihydrite and goethite

Addition of 2,6-DMHQ to the iron oxides produced IR spectra that showed clear spectral changes with increasing reaction time at pH 4.5 and 7.0. These changes indicated at least two surface complexes with different reaction kinetics. MCR-ALS resolved two main components (Figure 8). Component 1 (C1) was characterized by bands at 1385 and 1532 cm^{-1}, which increased steadily over time becoming the main component at the end of the experiment where 2,6-dimethoxybenzoquinone (2,6-DMBQ) should exist. An additional experiment with 2,6-DMBQ showed no or very low affinity for the iron oxide surfaces. Therefore, C1 was suggested to be an oxidation side-product with strong surface affinity. These results explained the incomplete recovery of 2,6-DMBQ indicated by the HPLC results.

Component 2 (C2) pre-dominated on surfaces during the first 20-30 min and the IR spectral features varied depending on the reaction conditions (Figure 8). At pH 4.5 and under aerobic conditions, C2 was identified as a semiquinone by the DFT calculations, primarily due to the lost absorbance at 1595 cm^{-1} and the strong intensity at 1500 cm^{-1}. Moreover, the DFT calculations indicated adsorption of a mixture of deprotonated and protonated semiquinones. The identification of the adsorbed semiquinone by the DFT calculations was supported by the HPLC results,

which indicated the presence of semiquinone when both redox forms of the quinone co-existed during the first 30 min of the experiment. This is in agreement with a comproportionation reaction[59,81] that can result in formation of semiquinone in the µM concentration range.[133] At pH 4.5 and under anaerobic conditions, C2 comparison with the DFT results as well as with model compound spectra suggested the existence of protonated 2,6-DMHQ with contribution from the semiquinone. The protonated 2,6-DMHQ surface species was also identified at pH 7.0 and under aerobic conditions.

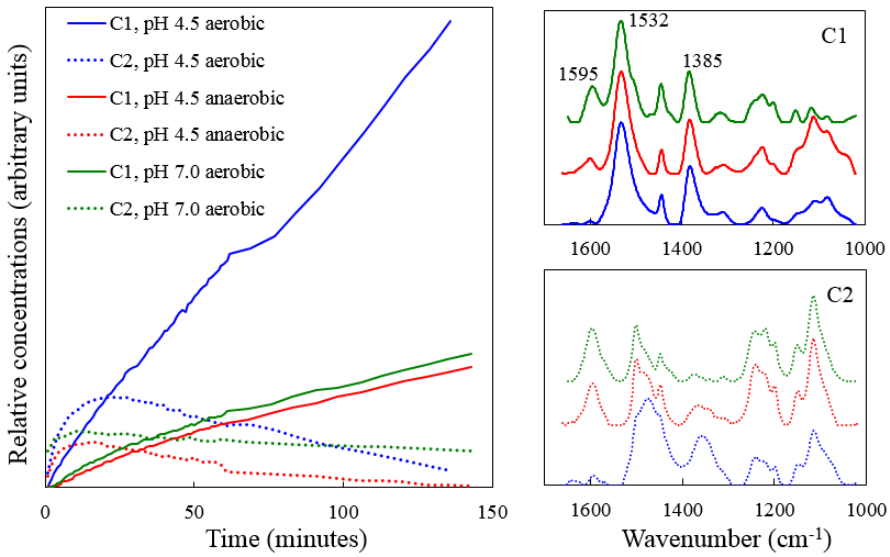

Figure 8. Multivariate curve resolution analysis of IR spectra of ferrihydrite during reaction with 2,6-DMHQ (total concentration = 9.9 µmol/m^2). IR data sets were collected every minute for approximately 140 min. The estimated MCR concentration profiles and the corresponding spectra are coded using the same color and line style.

The rate of hydroquinone autoxidation (R4) is increasing with increasing pH, and accordingly, with decreasing pK_a.[81] This was supported by the first order 2,6-DMHQ autoxidation rate constants, which increased from 6.8×10^{-4} min^{-1} at pH 4.0 to 2.0×10^{-2} min^{-1} at pH 7.0. Mechanisms that will promote deprotonation of hydroquinone, will therefore result in an increased oxidation rate. Several studies have shown that on iron oxides the deprotonated form of organic acids became more stable compared to the organic acids in bulk solution.[134–137] Accordingly, accumulation of 2,6-DMHQ at the positively charged interface possibly lowered the pK_a values of 2,6-DMHQ, and thereby increased the oxidation rate. The oxidation rate of hydroquinone can also be increased by a change in H_2Q electronic structure and/or by interactions between O_2 and Fe^{3+}.[138] The estimated pK_{a1} = 10.80 and pK_{a2} = 12.79 values of 2,6-DMHQ indicated that at pH 7.0 only a small fraction of the

deprotonated form will exist. Still, this can have a large effect on the oxidation kinetics.

At pH 4.5 and under aerobic conditions, the oxidation rates of 2,6-DMHQ by ferrihydrite and goethite were slower than at pH 7.0. This was in line with the pH effect just discussed and that 2,6-DMHQ oxidation rates mainly are controlled by the deprotonated species.

Fe^{2+} impact on redox reactions

In redox reactions, one 2,6-DMHQ molecule can donate two electrons and correspondingly reduce two Fe^{3+}. However, the results at pH 4.5 and under aerobic conditions and in the presence of iron oxides showed lower Fe^{2+} concentrations than expected from the 1 H_2Q: 2 Fe^{2+} ratio. At these reaction conditions, calculated ratios were ca. 1 H_2Q: 1 Fe^{2+} and 1 H_2Q: 0.08 Fe^{2+} in the presence of ferrihydrite and goethite, respectively. This indicated the contribution from catalytic oxidation (R5), particularly in the presence of goethite. At anaerobic conditions, higher concentrations of Fe^{2+} were measured, however Fe^{2+} concentrations came to a steady state with high amounts of 2,6-DMHQ still left in solution, especially with goethite.

Recently, Gorski *et al.*[139] demonstrated that the E_H of Fe^{3+} oxide/Fe^{2+} redox couple is decreasing with increasing Fe^{2+} concentration. Hence, E_H(Fe^{3+} oxide/ Fe^{2+}) will become lower than the E_H(HSQ/H_2Q) and/or E_H(Q/HSQ) at some point. Consequently, reductive dissolution (R6) will no longer be thermodynamically favorable. Using E_H values of ferrihydrite, goethite and 2,6-DMHQ,[140] approximately 100 μM and 1 mM Fe^{2+} can be reductively dissolved from goethite and ferrihydrite by 2,6-DMHQ (Figure 9). Approaching these Fe^{2+}concentrations, the E_H(Fe^{3+} oxide/Fe^{2+}) will drop below E_H(2,6-DMHQ/2,6-DMBQ), thus creating non-favorable thermodynamic conditions for reductive dissolution. The calculated values of E_H explained why at pH 4.5 and under anaerobic conditions only 80 μM Fe^{2+} was dissolved from goethite when ca. 75 % of 2,6-DMHQ remained in solution.

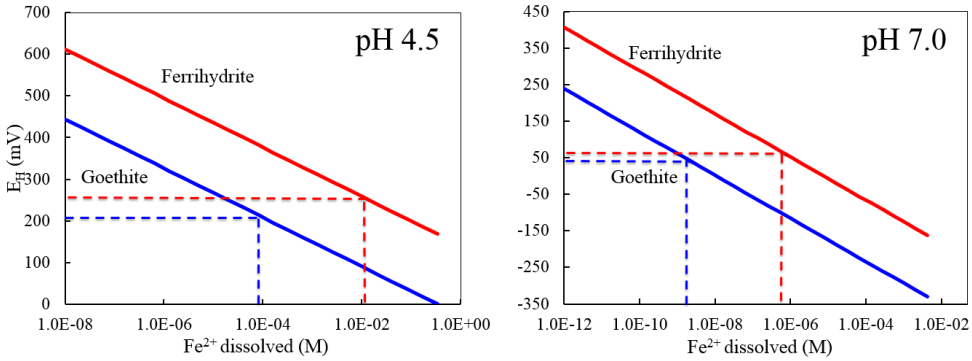

Figure 9. E_H of the Fe^{3+} oxide/Fe^{2+} redox couple as a funcion of dissolved Fe^{2+} concentrations in the presence of ferrihydrite and goethite. The solid lines were calculated according to Gorski *et al.*[139] The dashed lines represent E_H of the 2,6-DMBQ/2,6-DMHQ redox couple at the 2,6-DMHQ and 2,6-DMBQ concentrations after 240 min under anaerobic conditions calculated using the Nernst equation and the E_H^0 value from Huynh *et al.*[141]

Calculations at pH 7.0 indicated that reductive dissolution by 2,6-DMHQ/2,6-DMBQ redox couple can be achieved (Figure 9). At pH 7.0, the E_H of the iron oxides drops below the one-electron E_H(2,6-DMHQ/HSQ) at low Fe^{2+} concentrations, but the HSQ/2,6-DMBQ redox couple with a more negative E_H[81] should be able to dissolve iron oxide to a larger extent, provided the semiquinone is formed. It has been suggested that enzymes, such as laccases, can overcome the barrier of the one-electron reduction from 2,6-DMHQ to the semiquinone, thereby boosting the reduction efficiency of hydroquinones in biogeochemical systems.[54]

Similar results (i.e., similar 2,6-DMHQ oxidation pathways and H_2Q:Fe^{2+} ratios) were obtained by adding a lower concentration of 2,6-DMHQ to ferrihydrite and goethite (**Paper II**). In summary, these results illustrated that 2,6-DMHQ oxidation pathways were largely determined by E_H of the iron oxides and the O_2 concentration.

Impact of adsorbed molecules on the redox reactions

The study in **Paper I** was performed in a system free from strongly competing adsorbates. However, soil environments are rich in different organic and inorganic compounds with a strong affinity to adsorb to mineral surfaces. Thus, reactions similar to the 2,6-DMHQ reductive dissolution and catalytic oxidation are complicated by the influence of competing molecules. This was shown in the present studies where an adsorbed TPA probe (**Paper II**) and pre-adsorbed phosphate (**Paper III**) affected the 2,6-DMHQ oxidation pathways and the interactions between the 2,6-DMHQ and iron oxides.

Rapidly adsorbed and deprotonated outer-sphere TPA impacted the 2,6-DMHQ oxidation on the ferrihydrite and goethite surfaces in different ways (**Paper II**). In the presence of goethite, TPA adsorption inhibited the oxidation of 2,6-DMHQ under aerobic conditions. Accordingly, in the goethite system where catalytic oxidation (R5) predominated, TPA competed with the 2,6-DMHQ and O_2 surface species and inhibited the catalytic reaction (R5). In contrast, TPA adsorbed on the ferrihydrite surfaces increased the 2,6-DMHQ oxidation rate under both aerobic and anaerobic reaction conditions. Here the reductive dissolution (R6) was substantial, therefore these results indicated that TPA promotes this reaction. One explanation could be that the TPA adsorption reduced the positive surface charge and thereby favor proton adsorption. If this is the case and protonated surface sites are involved in the reductive dissolution reaction, this could be the reason why TPA increased the oxidation rates of 2,6-DMHQ.

The strong inner-sphere surface complexes of phosphate had a more pronounced inhibiting effect on the 2,6-DMHQ oxidation, especially in the presence of goethite (**Paper III**). For example, when the goethite surface was over-saturated with pre-adsorbed phosphate (total P_i 4 µmol/m^2), the oxidation rate of 2,6-DMHQ was close to the autoxidation rate (Figure 10). Similar to the results of TPA adsorption on goethite and ferrihydrite under anaerobic conditions, phosphate adsorption did not substantially interfere with reductive dissolution. Instead, phosphate adsorption mainly interfered with catalytic oxidation (R5), and increasing phosphate adsorption lead to markedly decreased oxidation rates of 2,6-DMHQ (Figure 10). These results are in line with the studies that showed that phosphate adsorption can decrease catalytic properties of various metal oxides.[117,142,143]

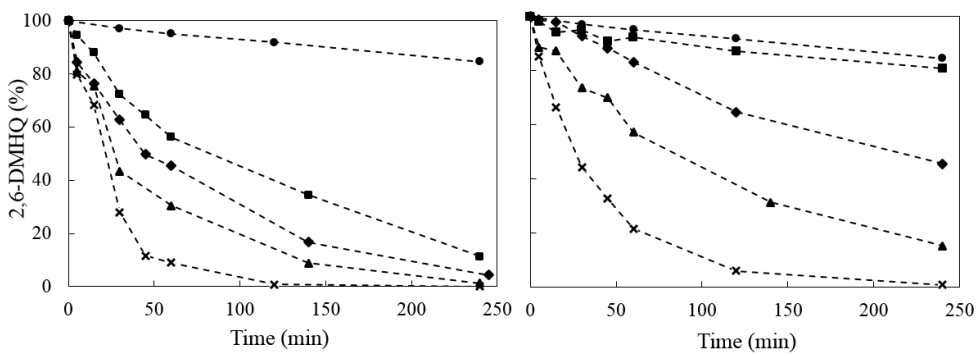

Figure 10. 2,6-DMHQ (1.5 µmol/m^2, 450 µM) oxidation in the absence and presence of different adsorbed phosphate (P_i) surface coverage onto ferrihydrite (left) and goethite (right) at pH 4.0. (●) autoxidation of 2,6-DMHQ, (×) phosphate free, (▲) 1 µmol P_i/m^2, (♦) 2 µmol P_i /m^2, (■) 4 µmol P_i /m^2.

In the 2,6-DMHQ-ferrihydrite systems where the reductive dissolution was an important pathway for 2,6-DMHQ oxidation, phosphate desorption was observed.

The bond strengths between Fe^{2+} bond and the surface, and between Fe^{2+} and phosphate were weaker than the corresponding Fe^{3+} bonds.[144] As a result, iron oxide reduction caused both Fe^{2+} and phosphate release into the bulk solution. Moreover, comparing phosphate desorption with different phosphate surface concentrations, results indicated that electron transfer likely occurred at surface sites that were not bound with phosphate.[145,146]

As mentioned above, at pH 4.0 and 4.5 and anaerobic conditions, adsorbed TPA and phosphate had low impact on the reductive dissolution reaction (R6), and a similar H_2Q: Fe^{2+} ratio as in the absence of adsorbed molecules was obtained. However the effects from TPA **(Paper II)** and phosphate on Fe^{2+} were much more dramatic (Figure 11).

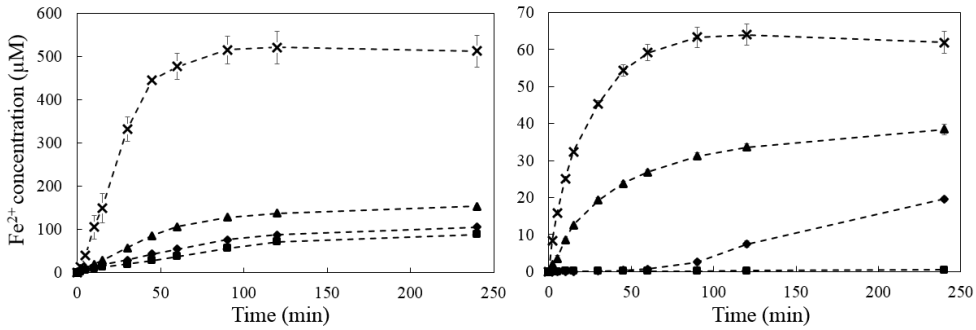

Figure 11. Ferrihydrite (left) and goethite (right) reductive dissolution by 2,6-DMHQ (450 µM, 1.5 µmol/m^2) at pH 4.0 in the absence and presence of 24 h pre-adsorbed phosphate. (×) phosphate free, (▲) 1 µmol P_i /m^2, (♦) 2 µmol P_i /m^2, (■) 4 µmol P_i /m^2.

The study of phosphate desorption from ferrihydrite and goethite surfaces (**Paper IV**) showed that surface electrostatic effects influence desorption mechanisms; for instance, increasing positive surface charge will decrease desorption of negatively charged phosphate ions. These findings suggested that adsorption of any organic or inorganic anion, such as small organic acids or oxyanions, will lower the surface charge and therefore influence the desorption rates of other charged surface species. Accordingly, adsorption of TPA and phosphate lowered the surface charge, and in turn slowed down the desorption rates of Fe^{2+} dissolved from the iron oxide surfaces. Furthermore, when catalytic oxidation of 2,6-DMHQ occurs, •OOH (R8 and R10) and H_2O_2 (R11) are formed.

$$H_2Q + O_2 \rightarrow HSQ + \bullet OOH \qquad (R10)$$

$$2\bullet OOH \rightarrow H_2O_2 \qquad (R11)$$

•OOH is known to adsorb on iron oxide surfaces,[147] and therefore, adsorption of anions should affect this species and the production of H_2O_2. This implies that such

anion adsorption will slow down Fe^{2+} desorption and could at the same time favor H_2O_2 formation, which will favor the Fenton reaction and generation of •OH radicals at iron oxide surface. This reasoning explains why lower concentrations of Fe^{2+} in solution were detected in the presence of adsorbed phosphate (Figure 11) and TPA **(Paper II)**. Pre-adsorbed phosphate also had further impact on the formation of •OH. With increasing phosphate surface coverage, a decrease in •OH formation rate was observed. This was related to the phosphate inhibition on the catalytic oxidation reaction (R5), which lowered the formation rate of H_2O_2 (R8, R10 and R11). Note, however, that direct quantitative comparison between experiments at low (under-saturated surfaces) and high (over-saturated surfaces) phosphate concentrations is difficult to interpret because surface TPA was out-competed by phosphate. For this reason, the efficiency of the TPA probe to capture •OH at the surfaces and in solution will vary with the total phosphate concentration.

At pH 7.0, 2,6-DMHQ was oxidized within 30 min in the presence of TPA and at all phosphate surface coverages. The predominating mechanism at this pH was catalytic oxidation that should be affected by TPA and phosphate competition according to the discussion above. However, with increasing pH and decreasing surface charge, the surface affinity of anions will decrease. Pure goethite has a point of zero charge (PZC) at ca. 9.5, while PZC of ferrihydrite is ca. 8.1.[122,148] Accordingly, lower phosphate adsorption was observed in the presence of ferrihydrite, thus free surface sites were available for catalytic oxidation of 2,6-DMHQ, which then explained the high 2,6-DMHQ catalytic oxidation rate. Higher phosphate adsorption was detected on the goethite surface at pH 7.0, implying a high competition between phosphate and 2,6-DMHQ. Yet, the 2,6-DMHQ first-order oxidation rate constant only decreased from 1.8×10^{-1} min^{-1} at pure goethite surface to 1.1×10^{-1} min^{-1} at 4 μmol P_i/m^2. It has been shown that adsorption of neutral molecules containing -OH functional groups, such as glucose, increase with increasing pH.[149] Therefore, 2,6-DMHQ adsorption might increase at pH 7.0 resulting in a high catalytic oxidation rate despite the presence of pre-adsorbed phosphate. To support this hypothesis, further studies of 2,6-DMHQ adsorption as function of pH and surface charge are needed.

As already noted, the catalytic oxidation of 2,6-DMHQ dominated at pH 7.0 and under aerobic conditions and 2,6-DMHQ was oxidized within 15-30 min. It follows that generation of H_2O_2 should take place within this time range. In the absence of competing anions, low concentrations of •OH were generated (Figure 12). Interestingly, when phosphate was added to the systems, the generation of •OH increased in several cases (Figure 12). Previous studies at neutral and basic pH values have shown that adsorption of various kinds of molecules on iron minerals can decrease H_2O_2 decomposition and favor •OH formation.[102,104] This would explain our observations in the phosphate-containing systems. These results raised the question if different surface sites are involved in H_2O_2 decomposition into H_2O

and O_2 or •OH. To increase the understanding of H_2O_2 reactions with iron minerals, more detailed surface spectroscopic studies are required.

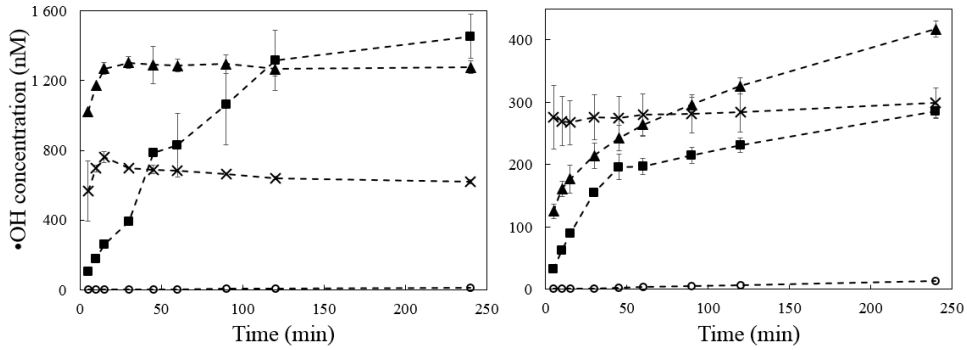

Figure 12. Hydroxyl radical production in presence of ferrihydrite (left) and goethite (right) by 2,6-DMHQ (450 µM, 1.5 µmol/m^2) in absence and presence of 24 h pre-adsorbed phosphate at different surface coverage concentrations at pH 7.0. (×) phosphate free, (▲) 1 µmol P_i /m^2, (■) 4 µmol P_i /m^2, (O) 450 µM H_2O_2.

Iron oxide interactions with DOM and DOM modified by P. involutus

During N acquisition *P. involutus* decomposes DOM into smaller and more polar molecules and concomitantly produces secondary metabolites containing aromatic and phenolic structures.[150] Indeed, the experiments with DOM decomposed by *P. involutus* revealed the formation of new compounds (**Paper V**). Compared to the initial DOM material (DOM_{ini}), the modified DOM extracted by ethyl acetate (DOM_{EtOAc}) showed increased amounts of molecules with aromatic and phenolic functional groups. Moreover, DOM_{EtOAc} fractions showed higher affinity towards iron oxide surfaces, thus supporting the hypothesis that organic matter (OM) decomposition contributes to the formation of OM-mineral associations and ultimately, to the SOM stabilization.

In the presence of ferrihydrite and goethite, DOM_{ini} displayed a low iron reducing activity, but this was increased considerably by the DOM_{EtOAc} fraction. At pH 4.0, DOM_{EtOAc} was more efficient in reductively dissolving ferrihydrite than goethite: Fe^{2+} concentrations were 3-4 times higher in the presence of ferrihydrite as compared to goethite after 240 min of reaction time. These results were in line with the higher reduction potential of ferrihydrite.[139] Moreover, the higher reductive dissolution of ferrihydrite was correlated to IR spectroscopic changes resolved by the MCR-ALS analysis that identified an IR band at ca. 1500 cm^{-1} that decreased with increasing reaction time. Previously, this IR band has been assigned to aromatic

secondary metabolites.[150] Therefore, these results suggested that these metabolites were involved in the redox reaction at the ferrihydrite surfaces.

Due to the fluorescence of DOM_{EtOAc}, it was not possible to determine if the DOM_{EtOAc} fraction contained secondary metabolites capable of producing H_2O_2 and thereby initiate the Fenton reaction. Instead, •OH formation and the impact of •OH on DOM was compared via two different types of experiments: (1) addition of DOM and H_2O_2 simultaneously to the iron oxides, or (2) pre-adsorption of DOM on the iron oxides for 24 h prior to H_2O_2 addition. In experiments conducted at 12 µmol TOC/m^2 of DOM, the iron oxide surfaces were partly saturated, thus free surface sites where available for H_2O_2 decomposition into •OH (R12) or O_2 and H_2O (R13).[91,101] In the absence of DOM, ferrihydrite can contribute to •OH formation via surface catalyzed degradation of H_2O_2 (R12), whereas in the presence of goethite, negligible formation of •OH was observed, indicating that goethite mainly promoted H_2O_2 decomposition into O_2 and H_2O.

$$H_2O_2 \xrightarrow[catalyst]{FeOOH} \bullet OH + OH^- \qquad \text{(R12)}$$

$$2H_2O_2 \xrightarrow[catalyst]{FeOOH} 2H_2O + O_2 \qquad \text{(R13)}$$

The addition of H_2O_2 to the DOM-iron oxide suspension resulted in immediate oxidation of Fe^{2+} and the generation of •OH above the background signal. Reductive dissolution of ferrihydrite by DOM_{EtOAc} resulted in higher Fe^{2+} concentrations, and thus generated the highest concentrations of •OH. Interestingly, with simultaneous mixing of H_2O_2, DOM_{EtOAc} and ferrihydrite, the •OH from the first reaction time point was close to the total iron concentration of DOM_{EtOAc} indicating an almost stoichiometric Fenton reaction. A different observation was made when H_2O_2 was added to the pre-equilibrated DOM-ferrihydrite systems where lower amounts of •OH were detected than expected from the Fenton stoichiometry. This was also accompanied by changes in the IR spectra of DOM_{ini}- and DOM_{EtOAc}-ferrihydrite (Figure 13). In both cases, the aromatic and phenolic bands at 1500 and 1280 cm^{-1} decreased, whereas a band at 1670 cm^{-1} increased over time. Several studies have shown that iron bioavailability is affected by complexation with organic matter. Moreover, complexation has been shown to inhibit Fe^{2+} oxidation.[151,152] During the parallel DOM adsorption and reductive dissolution reactions of ferrihydrite, a fraction of Fe^{2+} might form complexes with adsorbed DOM components.[151,152] A subsequent addition of H_2O_2 will result in the formation of •OH via Fe^{2+} oxidation in very close contact to the organic molecules. This would explain why the short-lived •OH was able to oxidize adsorbed DOM components. Moreover, the IR spectral changes indicated a decrease in bands characteristic of aromatic and phenolic compounds during this oxidation reaction, implying that some secondary

metabolites were consumed.[150] Hence, the overall results suggested that these types of fungal secondary metabolites act both as antioxidants and iron reductants. Molecules with antioxidant properties have been shown to inhibit oxidation of other DOM components, and therefore, they may contribute to partial DOM recalcitrance.[153,154]

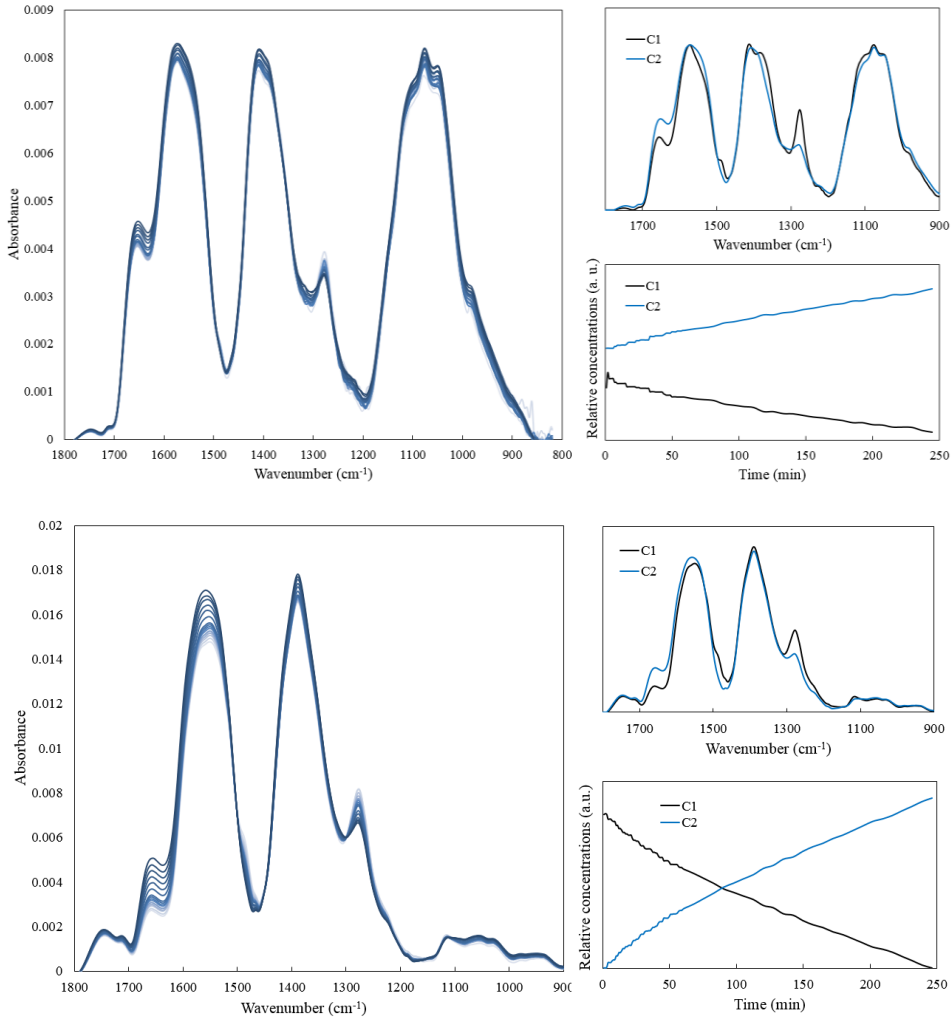

Figure 13. IR spectra of DOM_{ini} (top) and DOM_{EtOAc} (bottom) pre-adsorbed to ferrihydrite for 24 h after the addition of 100 μM H_2O_2 as a function of time at pH 4.0 and a total concentration of 12 μmol TOC/m^2 (left). MCR component spectra (top right) and MCR component concentrations (bottom right).

Possible implications for the soil environment

Oxidized quinones can be reduced to hydroquinones by several enzymes,[56] however, under aerobic conditions, oxidation of the model compound 2,6-DMHQ by iron oxides resulted in incomplete recovery of 2,6-DMBQ. If similar processes occur in soils, with each redox cycle between the hydroquinone and iron oxides, less quinones will be available for re-generation, and thereby less hydroquinones for generation of •OH. This would mean a continuous need for biosynthesis of hydroquinones by fungi in order to access the nutrients, if the processes were dependent on this type of •OH generation. Moreover, the results highlighted the importance of O_2 and clearly for the •OH generation to be effective O_2 needs to be constantly replenished, which also implies that it will be hampered under anaerobic microsites.

Incomplete oxidation to 2,6-DMBQ under aerobic conditions resulted in formation of oxidation side-products. Previous studies of similar systems involving other kinds of hydroquinones have shown a very diverse collection of reaction products, from polymers to CO_2.[87] CO_2 was not measured in our experimental systems, thus at the moment, it is not known whether the hydroquinone-iron oxide redox reactions will decompose organic compounds into CO_2 and impact the atmospheric CO_2 levels. Instead, the results showed that some of the reaction products were strongly bonded to the iron oxide surfaces. For this reason, SOM stability might be increased as a result of reactions between the organic iron reducing compounds and iron oxides.

The 2,6-DMHQ-promoted reductive dissolution of the iron oxides was shown to cause a transient desorption of strongly bonded phosphate ions. Thus, this redox reaction may favor phosphate bioavailability to plants and microbes, but at the same time it may also cause adverse effects because toxic elements, for example arsenic, also could be desorbed. As a consequence, arsenic contamination in aquatic environments could be aggravated.[32]

ISCO and AOPs techniques have been applied to degrade soil organic contaminants with phenolic and hydroquinone structures in the presence of iron-containing minerals and at neutral pH values.[96,155] Our results showed that the generation of •OH by 2,6-DMHQ-iron oxide reactions at pH 7.0 was boosted when the iron oxide nanoparticles were partly covered with an anionic ligand, such as phosphate ions. The pre-adsorbed phosphate shifted H_2O_2 decomposition into a higher generation of •OH. Thus co-adsorbed anions can possibly increase the efficiency of ISCO and AOPs mitigation techniques. Also, organic pollutants that are associated with iron oxide minerals may be oxidized into less toxic compounds through naturally occurring radical-based processes triggered by fungal secondary metabolites.

Broader implications of iron oxide nanoparticles

The development of nanomaterials and their applications have drastically increased during the 21st century. The unique properties of these nanomaterials provide useful and important advantages in various fields, such as medicine, agriculture, food industry.[156–158] With the increasing usage of nanomaterials, the terms "nano toxicity" and "nano safety" have also become more recognized, particularly in relation to O_2-dependent organisms.[159–162] Several studies have shown that not only free metal ions, but also the presence of nanoparticles are linked to increasing ROS levels.[163] An overproduction of ROS can damage and kill cells[164] and the most reactive of these species, •OH, can attack DNA directly.[165] ROS generation due the presence of nanoparticles has been correlated to their surface chemistry, particle size, crystal morphology, surface area, etc.[163] However, the fundamental reasons behind ROS overproduction by nanoparticles in biological systems are far from understood.

The overproduction of ROS is known to lead to oxidative stress, i.e., biological systems loses their ability to neutralize ROS and as a result, cells fail to sustain physiologically redox-regulated functions.[166] It has been shown that oxidative stress is connected with (aging) diseases, such as diabetes, cancer, Alzheimer's and Parkinson's disease, multiple sclerosis, etc.[167–171] In contrast, ROS can be used for therapeutic purposes because cancer cells are killed by initiating oxidative stress in cancerous cells.[169,172]

This PhD project provided insight to the •OH production in the presence of iron oxide nanoparticles via different reaction pathways, such as the Fenton and Haber-Weiss reactions. These are processes that might cause nano toxicity of the iron oxides but little is known about these effects. In particular, there is a limited understanding on what damage soil organisms could experience under increased exposure of ROS and/or nanomaterials, despite the abundance of iron oxide particles in soils.[173]

The results from this thesis showed that high concentrations of •OH can be generated by organic reductants in the presence of iron oxides, and that this will have an impact on SOM decomposition. At the same time, SOM contains phenolic compounds that can act as antioxidants in a wide E_H range outside the microorganism. Thus, antioxidant properties of phenolic compounds in SOM can not only defend microorganisms from ROS attack, but also inhibit oxidative SOM transformations, and therefore increase SOM stability.[153]

Conclusions and future perspectives

This thesis focused on the reactions between iron oxide nanoparticles of different crystallinities (i.e. ferrihydrite and goethite) and organic compounds with iron-reducing capacity. Two questions that were addressed and answered were whether a hydroquinone (2,6-DMHQ) and DOM, as well as DOM modified by the ECM fungus *P. involutus,* could reductively dissolve the iron the oxides and create favorable conditions for •OH generation via Fenton chemistry. Moreover, the sensitivity of these reactions to the experimental conditions, such as pH and O_2, levels were investigated. In summary, the results of this PhD project demonstrated that:

- 2,6-DMHQ oxidation pathways were determined by pH, E_H of the iron oxides, O_2 concentration and competitive adsorption of inorganic and organic molecules;
- Increasing Fe^{2+} concentrations decreased the $E_H(Fe^{3+}$ oxide/$Fe^{2+})$, which limited the 2,6-DMHQ-promoted reduction, primarily of goethite;
- Under aerobic reaction conditions the 2,6-DMHQ-iron oxide reactions initiated the Fenton reaction via reductive dissolution and catalytic oxidation that produced the Fenton reagents Fe^{2+} and H_2O_2;
- At pH 4.0 and 4.5, the adsorption of anionic inorganic and organic molecules lowered the iron oxide surface charge, which favored the Fenton reaction at the iron oxide surfaces;
- At pH 7.0, H_2O_2 decomposition into •OH or O_2 and H_2O_2 was affected by the adsorption of anionic molecules on the iron oxide surfaces;
- Ferrihydrite and goethite nanoparticles were reductively dissolved by DOM modified by *P. involutus*;
- *P. involutus* secondary metabolites can serve as antioxidants and iron oxide reductants

The laboratory experiments of this PhD project were conducted in the presence of the common and well-characterized iron oxides: ferrihydrite and goethite. However, in soils, iron is also found in a range of different minerals as well as complexed to SOM. The presented results showed that the redox reactions were influenced by the

iron oxide properties including E_H. It would therefore be of great interest to expand these studies to different iron minerals including real soil mineral assemblages in order to further understand the impact fungal secondary metabolites.

The reactions under aerobic conditions indicated the formation of oxidation side-products that were strongly adsorbed to iron oxide surfaces. This suggests that such reactions can lead to the stabilization of C in soil. On the other hand, similar studies between hydroquinone-like molecules and metal oxides have detected the release of CO_2.[87] Future studies of redox-active microbial metabolites and iron oxides surfaces should therefore include quantification of the processes leading to CO_2 emissions and those leading to the stabilization of new OM-mineral aggregates, and how these processes are affected by environmental parameters.

The study on DOM modified by *P. involutus* was performed in complex organic compound mixture and the results indicated several reaction pathways between DOM_{EtOAc}, H_2O_2 and the iron oxides. In order to further understand the consequences of DOM modifications for OM-mineral interactions additional fractionation, purification and characterization are needed. This will provide a deeper insight into the precise roles of individual compounds/compound classes and how they contribute to non-enzymatic •OH generation as well as to OM-mineral stability.

References

(1) Moore, M. N. Do Nanoparticles Present Ecotoxicological Risks for the Health of the Aquatic Environment? *Environ. Int.* **2006**, *32*, 967–976.

(2) Handy, R. D.; Owen, R.; Valsami-Jones, E. The Ecotoxicology of Nanoparticles and Nanomaterials: Current Status, Knowledge Gaps, Challenges, and Future Needs. *Ecotoxicology* **2008**, *17*, 315–325.

(3) Gupta, A. K.; Gupta, M. Synthesis and Surface Engineering of Iron Oxide Nanoparticles for Biomedical Applications. *Biomaterials* **2005**, *26*, 3995–4021.

(4) Corot, C.; Robert, P.; Idée, J.-M.; Port, M. Recent Advances in Iron Oxide Nanocrystal Technology for Medical Imaging. *Adv. Drug Deliv. Rev.* **2006**, *58*, 1471–1504.

(5) Jain, T. K.; Morales, M. A.; Sahoo, S. K.; Leslie-Pelecky, D. L.; Labhasetwar, V. Iron Oxide Nanoparticles for Sustained Delivery of Anticancer Agents. *Mol. Pharm.* **2005**, *2*, 194–205.

(6) Babes, L.; Denizot, B.; Tanguy, G.; Le Jeune, J. J.; Jallet, P. Synthesis of Iron Oxide Nanoparticles Used as MRI Contrast Agents: A Parametric Study. *J. Colloid Interface Sci.* **1999**, *212*, 474–482.

(7) Mahmoudi, M.; Sant, S.; Wang, B.; Laurent, S.; Sen, T. Superparamagnetic Iron Oxide Nanoparticles (SPIONs): Development, Surface Modification and Applications in Chemotherapy. *Adv. Drug Deliv. Rev.* **2011**, *63*, 24–46.

(8) Figuerola, A.; Di Corato, R.; Manna, L.; Pellegrino, T. From Iron Oxide Nanoparticles towards Advanced Iron-Based Inorganic Materials Designed for Biomedical Applications. *Pharmacol. Res.* **2010**, *62*, 126–143.

(9) Laurent, S.; Dutz, S.; Häfeli, U. O.; Mahmoudi, M. Magnetic Fluid Hyperthermia: Focus on Superparamagnetic Iron Oxide Nanoparticles. *Adv. Colloid Interface Sci.* **2011**, *166*, 8–23.

(10) Kim, E. H.; Ahn, Y.; Lee, H. S. Biomedical Applications of Superparamagnetic Iron Oxide Nanoparticles Encapsulated within Chitosan. *J. Alloys Compd.* **2007**, *434*, 633–636.

(11) Dilnawaz, F.; Singh, A.; Mohanty, C.; Sahoo, S. K. Dual Drug Loaded Superparamagnetic Iron Oxide Nanoparticles for Targeted Cancer Therapy. *Biomaterials* **2010**, *31*, 3694–3706.

(12) Portet, D.; Denizot, B.; Rump, E.; Lejeune, J.-J.; Jallet, P. Nonpolymeric Coatings of Iron Oxide Colloids for Biological Use as Magnetic Resonance Imaging Contrast Agents. *J. Colloid Interface Sci.* **2001**, *238*, 37–42.

(13) Xu, P.; Zeng, G. M.; Huang, D. L.; Feng, C. L.; Hu, S.; Zhao, M. H.; Lai, C.; Wei,

Z.; Huang, C.; Xie, G. X.; et al. Use of Iron Oxide Nanomaterials in Wastewater Treatment: A Review. *Sci. Total Environ.* **2012**, *424*, 1–10.

(14) Qu, X.; Alvarez, P. J. J. Applications of Nanotechnology in Water and Wastewater Treatment. *Water Res.* **2013**, *47*, 3931–3946.

(15) Zargar, B.; Parham, H.; Hatamie, A. Fast Removal and Recovery of Amaranth by Modified Iron Oxide Magnetic Nanoparticles. *Chemosphere* **2009**, *76*, 554–557.

(16) Hua, M.; Zhang, S.; Pan, B.; Zhang, W.; Lv, L.; Zhang, Q. Heavy Metal Removal from Water/Wastewater by Nanosized Metal Oxides: A Review. *J. Hazard. Mater.* **2012**, *211*, 317–331.

(17) Shahwan, T.; Abu Sirriah, S.; Nairat, M.; Boyacı, E.; Eroğlu, A. E.; Scott, T. B.; Hallam, K. R. Green Synthesis of Iron Nanoparticles and their Application as a Fenton-Like Catalyst for the Degradation of Aqueous Cationic and Anionic Dyes. *Chem. Eng. J.* **2011**, *172*, 258–266.

(18) Parham, H.; Zargar, B.; Shiralipour, R. Fast and Efficient Removal of Mercury from Water Samples using Magnetic Iron Oxide Nanoparticles Modified with 2-Mercaptobenzothiazole. *J. Hazard. Mater.* **2012**, *205*, 94–100.

(19) Teja, A. S.; Koh, P.-Y. Synthesis, Properties, and Applications of Magnetic Iron Oxide Nanoparticles. *Prog. Cryst. Growth Charact. Mater.* **2009**, *55*, 22–45.

(20) Kim, D. K.; Zhang, Y.; Voit, W.; Rao, K. V.; Muhammed, M. Synthesis and Characterization of Surfactant-Coated Superparamagnetic Monodispersed Iron Oxide Nanoparticles. *J. Magn. Magn. Mater.* **2001**, *225*, 30–36.

(21) Mak, S.-Y.; Chen, D.-H. Fast Adsorption of Methylene Blue on Polyacrylic Acid-Bound Iron Oxide Magnetic Nanoparticles. *Dye. Pigment.* **2004**, *61*, 93–98.

(22) Kaushik, A.; Khan, R.; Solanki, P. R.; Pandey, P.; Alam, J.; Ahmad, S.; Malhotra, B. D. Iron Oxide Nanoparticles–Chitosan Composite based Glucose Biosensor. *Biosens. Bioelectron.* **2008**, *24*, 676–683.

(23) Cao, M.; Li, Z.; Wang, J.; Ge, W.; Yue, T.; Li, R.; Colvin, V. L.; Yu, W. W. Food Related Applications of Magnetic Iron Oxide Nanoparticles: Enzyme Immobilization, Protein Purification, and Food Analysis. *Trends Food Sci. Technol.* **2012**, *27*, 47–56.

(24) Maity, D.; Agrawal, D. C. Synthesis of Iron Oxide Nanoparticles under Oxidizing Environment and their Stabilization in Aqueous and Non-Aqueous Media. *J. Magn. Magn. Mater.* **2007**, *308*, 46–55.

(25) Li, P.; Miser, D. E.; Rabiei, S.; Yadav, R. T.; Hajaligol, M. R. The Removal of Carbon Monoxide by Iron Oxide Nanoparticles. *Appl. Catal. B Environ.* **2003**, *43*, 151–162.

(26) Luengo, C.; Brigante, M.; Antelo, J.; Avena, M. Kinetics of Phosphate Adsorption on Goethite: Comparing Batch Adsorption and ATR-IR Measurements. *J. Colloid Interface Sci.* **2006**, *300*, 511–518.

(27) Persson, P.; Nilsson, N.; Sjöberg, S. Structure and Bonding of Orthophosphate Ions at the Iron Oxide–Aqueous Interface. *J. Colloid Interface Sci.* **1996**, *177*, 263–275.

(28) Loring, J. S.; Sandström, M. H.; Norén, K.; Persson, P. Rethinking Arsenate Coordination at the Surface of Goethite. *Chem. - A Eur. J.* **2009**, *15*, 5063–5072.

(29) Franzblau, R. E.; Daughney, C. J.; Moreau, M.; Weisener, C. G. Selenate Adsorption to Composites of Escherichia coli and Iron Oxide during the Addition, Oxidation, and Hydrolysis of Fe(II). *Chem. Geol.* **2014**, *383*, 180–193.

(30) Rath, S. S.; Sinha, N.; Sahoo, H.; Das, B.; Mishra, B. K. Molecular Modeling Studies of Oleate Adsorption on Iron Oxides. *Appl. Surf. Sci.* **2014**, *295*, 115–122.

(31) Buckley, A. N.; Parker, G. K. Adsorption of n-Octanohydroxamate Collector on Iron Oxides. *Int. J. Miner. Process.* **2013**, *121*, 70–89.

(32) Erbs, J. J.; Berquó, T. S.; Reinsch, B. C.; Lowry, G. V.; Banerjee, S. K.; Penn, R. L. Reductive Dissolution of Arsenic-Bearing Ferrihydrite. *Geochim. Cosmochim. Acta* **2010**, *74*, 3382–3395.

(33) Yuan, Z.; Zhang, D.; Wang, S.; Xu, L.; Wang, K.; Song, Y.; Xiao, F.; Jia, Y. Effect of Hydroquinone-Induced Iron Reduction on the Stability of Scorodite and Arsenic Mobilization. *Hydrometallurgy* **2016**, *164*, 228–237.

(34) Anschutz, A. J.; Penn, R. L. Reduction of Crystalline Iron(III) Oxyhydroxides Using Hydroquinone: Influence of Phase and Particle Size. *Geochem. Trans.* **2005**, *6*, 60–66.

(35) Davranche, M.; Bollinger, J.-C. Release of Metals from Iron Oxyhydroxides under Reductive Conditions: Effect of Metal/Solid Interactions. *J. Colloid Interface Sci.* **2000**, *232*, 165–173.

(36) Wolf, M.; Kappler, A.; Jiang, J.; Meckenstock, R. U. Effects of Humic Substances and Quinones at Low Concentrations on Ferrihydrite Reduction by Geobacter metallireducens. *Environ. Sci. Technol.* **2009**, *43*, 5679–5685.

(37) Erbs, J. J.; Gilbert, B.; Penn, R. L. Influence of Size on Reductive Dissolution of Six-Line Ferrihydrite. *J. Phys. Chem. C* **2008**, *112*, 12127–12133.

(38) Kung, K.-H.; McBride, M. B. Electron Transfer Processes Between Hydroquinone and Iron Oxides. *Clays Clay Miner.* **1988**, *36*, 303–309.

(39) LaKind, J. S.; Stone, A. T. Reductive Dissolution of Goethite by Phenolic Reductants. *Geochim. Cosmochim. Acta* **1989**, *53*, 961–971.

(40) Ortiz de la Plata, G. B.; Alfano, O. M.; Cassano, A. E. Decomposition of 2-Chlorophenol Employing Goethite as Fenton Catalyst. I. Proposal of a Feasible, Combined Reaction Scheme of Heterogeneous and Homogeneous Reactions. *Appl. Catal. B Environ.* **2010**, *95*, 1–13.

(41) Jia, Y.; Demopoulos, G. P. Adsorption of Arsenate onto Ferrihydrite from Aqueous Solution: Influence of Media (Sulfate vs Nitrate), Added Aypsum, and pH Alteration. *Environ. Sci. Technol.* **2005**, *39*, 9523–9527.

(42) Goh, K. H.; Lim, T. T. Geochemistry of Inorganic Arsenic and Selenium in a Tropical Soil: Effect of Reaction Time, pH, and Competitive Anions on Arsenic and Selenium Adsorption. *Chemosphere* **2004**, *55*, 849–859.

(43) Falkowski, P.; Scholes, R. J.; Boyle, E.; Canadell, J.; Canfield, D.; Elser, J.; Gruber, N.; Hibbard, K.; Högberg, P.; Linder, S.; et al. The Global Carbon Cycle: A Test of Our Knowledge of Earth as a System. *Science (80-.).* **2000**, *290*, 291–296.

(44) Schmidt, M. W. I.; Torn, M. S.; Abiven, S.; Dittmar, T.; Guggenberger, G.; Janssens, I. A.; Kleber, M.; Kogel-Knabner, I.; Lehmann, J.; Manning, D. A. C.; et al.

Persistence of Soil Organic Matter as an Ecosystem Property. *Nature* **2011**, *478*, 49–56.

(45) Torn, M. S.; Trumbore, S. E.; Chadwick, O. A.; Vitousek, P. M.; Hendrick, D. M. Mineral Control of Soil Organic Carbon Storage and Turnover. *Nature* **1997**, *389*, 170–173.

(46) Mikutta, R.; Kleber, M.; Torn, M. S.; Jahn, R. Stabilization of Soil Organic Matter: Association with Minerals or Chemical Recalcitrance? *Biogeochemistry* **2006**, *77*, 25–56.

(47) Baldock, J. A.; Skjemstad, J. O. Role of the Soil Matrix and Minerals in Protecting Natural Organic Materials Against Biological Attack. *Org. Geochem.* **2000**, *31*, 697–710.

(48) Sollins, P.; Homann, P.; Caldwell, B. A. Stabilization and Destabilization of Soil Organic Matter: Mechanisms and Controls. *Geoderma* **1996**, *74*, 65–105.

(49) Von Lützow, M.; Kögel-Knabner, I.; Ludwig, B.; Matzner, E.; Flessa, H.; Ekschmitt, K.; Guggenberger, G.; Marschner, B.; Kalbitz, K. Stabilization Mechanisms of Organic Matter in Four Temperate Soils: Development and Application of a Conceptual Model. *J. Plant Nutr. Soil Sci.* **2008**, *171*, 111–124.

(50) Wymelenberg, A. Vanden; Gaskell, J.; Mozuch, M.; Sabat, G.; Ralph, J.; Skyba, O.; Mansfield, S. D.; Blanchette, R. A.; Martinez, D.; Grigoriev, I.; et al. Comparative Transcriptome and Secretome Analysis of Wood Decay Fungi Postia placenta and Phanerochaete chrysosporium. *Appl. Environ. Microbiol.* **2010**, *76*, 3599–3610.

(51) Newcombe, D.; Paszczynski, A.; Gajewska, W.; Kröger, M.; Feis, G.; Crawford, R. Production of Small Molecular Weight Catalysts and the Mechanism of Trinitrotoluene Degradation by Several Gloeophyllum Species. *Enzyme Microb. Technol.* **2002**, *30*, 506–517.

(52) Baldrian, P.; Valášková, V. Degradation of Cellulose by Basidiomycetous Fungi. *FEMS Microbiol. Rev.* **2008**, *32*, 501–521.

(53) Jensen, K. A.; Houtman, C. J.; Ryan, Z. C.; Hammel, K. E. Pathways for Extracellular Fenton Chemistry in the Brown Rot Basidiomycete Gloeophyllum trabeum. *Appl. Environ. Microbiol.* **2001**, *67*, 2705–2711.

(54) Wei, D.; Houtman, C. J.; Kapich, A. N.; Hunt, C. G.; Cullen, D.; Hammel, K. E. Laccase and Its Role in Production of Extracellular Reactive Oxygen Species during Wood Decay by the Brown Rot Basidiomycete Postia Placenta. *Appl. Environ. Microbiol.* **2010**, *76*, 2091–2097.

(55) Korripally, P.; Timokhin, V. I.; Houtman, C. J.; Mozuch, M. D.; Hammel, K. E. Evidence from Serpula lacrymans that 2,5-Dimethoxyhydroquinone is a Lignocellulolytic Agent of Divergent Brown Rot Basidiomycetes. *Appl. Environ. Microbiol.* **2013**, *79*, 2377–2383.

(56) Kerem, Z.; Jensen, K. A.; Hammel, K. E. Biodegradative Mechanism of the Brown Rot Basidiomycete Gloeophyllum Trabeum: Evidence for an Extracellular Hydroquinone-Driven Fenton Reaction. *FEBS Lett.* **1999**, *446*, 49–54.

(57) Shimokawa, T.; Nakamura, M.; Hayashi, N.; Ishihara, M. Production of 2,5-Dimethoxyhydroquinone by the Brown-Rot Fungus Serpula lacrymans to Drive Extracellular Fenton Reaction. *Holzforschung* **2004**, *58*, 305–310.

(58) Cory, R. M.; McKnight, D. M. Fluorescence Spectroscopy Reveals Ubiquitous Presence of Oxidized and Reduced Quinones in Dissolved Organic Matter. *Environ. Sci. Technol.* **2005**, *39*, 8142–8149.

(59) Uchimiya, M.; Stone, A. T. Reversible Redox Chemistry of Quinones: Impact on Biogeochemical Cycles. *Chemosphere* **2009**, *77*, 451–458.

(60) Cornell, R. M.; Schwertmann, U. *The Iron Oxides*; Wiley-VCH, 2003.

(61) Schwertmann, U.; Cornell, R. M. *Iron Oxides in the Laboratory: Preparation and Characterization*; Wiley-VCH: Weinheim, 2000.

(62) Taylor, K. G.; Konhauser, K. O. Iron In Earth Surface systems: A Major Player in Chemical and Biological Processes. *Elements* **2011**, *7*, 83–88.

(63) Robin, A.; Vansuyt, G.; Hinsinger, P.; Meyer, J. M.; Briat, J. F.; Lemanceau, P. Iron Dynamics in the Rhizosphere. Consequences for Plant Health and Nutrition. *Adv. Agron.* **2008**, *99*, 183–225.

(64) Lemanceau, P.; Expert, D.; Gaymard, F.; Bakker, P. A. H. M.; Briat, J. F. Role of Iron in Plant-Microbe Interactions. *Adv. Bot. Res.* **2009**, *51*, 491–549.

(65) Polubesova, T.; Eldad, S.; Chefetz, B. Adsorption and Oxidative Transformation of Phenolic Acids by Fe(III)-Montmorillonite. *Environ. Sci. Technol.* **2010**, *44*, 4203–4209.

(66) Uchimiya, M.; Stone, A. T. Redox Reactions between Iron and Quinones: Thermodynamic Constraints. *Geochim. Cosmochim. Acta* **2006**, *70*, 1388–1401.

(67) Sugumaran, M. Quinone Methide Sclerotization: A Revised Mechanism for β-Sclerotization of Insect Cuticle. *Bioorg. Chem.* **1987**, *15*, 194–211.

(68) Sánchez, C. Lignocellulosic Residues: Biodegradation and Bioconversion by Fungi. *Biotechnol. Adv.* **2009**, *27*, 185–194.

(69) Ona-Nguema, G.; Morin, G.; Juillot, F.; Calas, G.; Brown, G. E. EXAFS Analysis of Arsenite Adsorption onto Two-Line Ferrihydrite, Hematite, Goethite, and Lepidocrocite. *Environ. Sci. Technol.* **2005**, *39*, 9147–9155.

(70) Stachowicz, M.; Hiemstra, T.; van Riemsdijk, W. H. Multi-Competitive Interaction of As(III) and As(V) Oxyanions with Ca2+, Mg2+, PO3- 4, and CO2-3 Ions on Goethite. *J. Colloid Interface Sci.* **2008**, *320*, 400–414.

(71) Gallegos-Garcia, M.; Ramírez-Muñiz, K.; Song, S. Arsenic Removal from Water by Adsorption Using Iron Oxide Minerals as Adsorbents: A Review. *Miner. Process. Extr. Metall. Rev.* **2012**, *33*, 301–315.

(72) Magario, I.; García Einschlag, F. S.; Rueda, E. H.; Zygadlo, J.; Ferreira, M. L. Mechanisms of Radical Generation in the Removal of Phenol Derivatives and Pigments Using Different Fe-Based Catalytic Systems. *J. Mol. Catal. A Chem.* **2012**, *352*, 1–20.

(73) Soil Organic Matter Characterization. In *Carbon and Nitrogen in the Terrestrial Environment*; Springer Netherlands: Dordrecht, 2008; pp 81–111.

(74) Högberg, P.; Read, D. J. Towards a more Plant Physiological Perspective on Soil Ecology. *Trends Ecol. Evol.* **2006**, *21*, 548–554.

(75) Read, D. J.; Leake, J. R.; Perez-Moreno, J. Mycorrhizal Fungi as Drivers of Ecosystem Processes in Heathland and Boreal Forest Biomes. *Can. J. Bot.* **2004**, *82*,

1243–1263.

(76) Rineau, F.; Roth, D.; Shah, F.; Smits, M.; Johansson, T.; Canbäck, B.; Olsen, P. B.; Persson, P.; Grell, M. N.; Lindquist, E.; et al. The Ectomycorrhizal Fungus Paxillus Involutus Converts Organic Matter in Plant Litter Using a Trimmed Brown-Rot Mechanism Involving Fenton Chemistry. *Environ. Microbiol.* **2012**, *14*, 1477–1487.

(77) Green, F.; Larsen, M. J.; Winandy, J. E.; Highley, T. L. Role of Oxalic Acid in Incipient Brown-Rot Decay. *Mater. und Org.* **1991**, *26*, 191–213.

(78) Park, J. S.; Wood, P. M.; Davies, M. J.; Gilbert, B. C.; Whitwood, a C. A Kinetic and ESR Investigation of Iron(II) Oxalate Oxidation by Hydrogen Peroxide and Dioxygen as a Source of Hydroxyl Radicals. *Free Radic. Res.* **1997**, *27*, 447–458.

(79) Shah, F.; Schwenk, D.; Nicolás, C.; Persson, P.; Hoffmeister, D.; Tunlid, A. Involutin Is an Fe(3+) Reductant Secreted by the Ectomycorrhizal Fungus Paxillus involutus during Fenton-Based Decomposition of Organic Matter. *Appl. Environ. Microbiol.* **2015**, *81*, 8427–8433.

(80) Paszczynski, A.; Crawford, R.; Funk, D.; Goodell, B. De Novo Synthesis of 4,5-dimethoxycatechol and 2, 5-dimethoxyhydroquinone by the Brown Rot Fungus Gloeophyllum trabeum. *Appl. Environ. Microbiol.* **1999**, *65*, 674–679.

(81) Song, Y.; Buettner, G. R. Thermodynamic and Kinetic Considerations for the Reaction of Semiquinone Radicals to Form Superoxide and Hydrogen Peroxide. *Free Radic. Biol. Med.* **2010**, *49*, 919–962.

(82) Stack, A. G.; Eggleston, C. M.; Engelhard, M. H. Reaction of Hydroquinone with Hematite: I. Study of Adsorption by Electrochemical-Scanning Tunneling Microscopy and X-Ray Photoelectron Spectroscopy. *J. Colloid Interface Sci.* **2004**, *274*, 433–441.

(83) Stack, A. G.; Rosso, K. M.; Smith, D. M. A.; Eggleston, C. M. Reaction of Hydroquinone with Hematite: II. Calculated Electron-Transfer Rates and Comparison to the Reductive Dissolution Rate. *J. Colloid Interface Sci.* **2004**, *274*, 442–450.

(84) Yong, R. N.; Desjardins, S.; Farant, J. P.; Simon, P. Influence of pH and Exchangeable Cation on Oxidation of Methylphenols by a Montmorillonite Clay. *Appl. Clay Sci.* **1997**, *12*, 93–110.

(85) Wang, M. C.; Huang, P. M. Catalytic Power of Nontronite, Kaolinite and Quartz and their Reaction Sites in the Formation of Hydroquinone-Derived Polymers. *Appl. Clay Sci.* **1989**, *4*, 43–57.

(86) Sawhney, B.; Kozloski, R.; Isaacson, P.; Gent, M. Polymerization of 2,6-Dimethylphenol on Smectite Surfaces. *Clays Clay Miner.* **1984**, *32*, 108–114.

(87) Chen, Y. M.; Tsao, T. M.; Liu, C. C.; Huang, P. M.; Wang, M. K. Polymerization of Catechin Catalyzed by Mn-, Fe- and Al-Oxides. *Colloids Surfaces B Biointerfaces* **2010**, *81*, 217–223.

(88) Liu, H.; Bruton, T. A.; Li, W.; Buren, J. Van; Prasse, C.; Doyle, F. M.; Sedlak, D. L. Oxidation of Benzene by Persulfate in the Presence of Fe(III)- and Mn(IV)-Containing Oxides: Stoichiometric Efficiency and Transformation Products. *Environ. Sci. Technol.* **2016**, *50*, 890–898.

(89) He, J.; Yang, X.; Men, B.; Bi, Z.; Pu, Y.; Wang, D. Heterogeneous Fenton Oxidation

of Catechol and 4-Chlorocatechol Catalyzed by Nano-Fe3O4: Role of the Interface. *Chem. Eng. J.* **2014**, *258*, 433–441.

(90) Benitez, F. J.; Real, F. J.; Acero, J. L.; Leal, A. I.; Garcia, C. Gallic Acid Degradation in Aqueous Solutions by UV/H2O2 Treatment, Fenton's Reagent and the Photo-Fenton System. *J. Hazard. Mater.* **2005**, *126*, 31–39.

(91) He, J.; Yang, X.; Men, B.; Wang, D. Interfacial Mechanisms of Heterogeneous Fenton Reactions Catalyzed by Iron-Based Materials: A Review. *J. Environ. Sci.* **2016**, *39*, 97–109.

(92) Wu, H.; Yin, J. J.; Wamer, W. G.; Zeng, M.; Lo, Y. M. Reactive Oxygen Species-Related Activities of Nano-Iron Metal and Nano-Iron Oxides. *J. Food Drug Anal.* **2014**, *22*, 86–94.

(93) Wang, B.; Yin, J. J.; Zhou, X.; Kurash, I.; Chai, Z.; Zhao, Y.; Feng, W. Physicochemical Origin for Free Radical Generation of Iron Oxide Nanoparticles in Biomicroenvironment: Catalytic Activities Mediated by Surface Chemical States. *J. Phys. Chem. C* **2013**, *117*, 383–392.

(94) Lin, S.-S.; Gurol, M. D. Catalytic Decomposition of Hydrogen Peroxide on Iron Oxide: Kinetics, Mechanism, and Implications. *Environ. Sci. Technol.* **1998**, *32*, 1417–23.

(95) Garrido-Ramírez, E. G.; Theng, B. K. G.; Mora, M. L. Clays and Oxide Minerals as Catalysts and Nanocatalysts in Fenton-like Reactions - A Review. *Appl. Clay Sci.* **2010**, *47*, 182–192.

(96) Pignatello, J. J.; Oliveros, E.; MacKay, A. Advanced Oxidation Processes for Organic Contaminant Destruction Based on the Fenton Reaction and Related Chemistry. *Crit. Rev. Environ. Sci. Technol.* **2006**, *36*, 1–84.

(97) Wilson, S. C.; Jones, K. C. Bioremediation of Soil Contaminated with Polynuclear Aromatic hydrocarbons (PAHs): A Review. *Environ. Pollut.* **1993**, *81*, 229–249.

(98) Wang, N.; Zheng, T.; Zhang, G.; Wang, P. A Review on Fenton-like Processes for Organic Wastewater Treatment. *J. Environ. Chem. Eng.* **2016**, *4*, 762–787.

(99) Petigara, B. R.; Blough, N. V.; Mignerey, A. C. Mechanisms of Hydrogen Peroxide Decomposition in Soils. *Environ. Sci. Technol.* **2002**, *36*, 639–645.

(100) Kwan, W. P.; Voelker, B. M. Decomposition of Hydrogen Peroxide and Organic Compounds in the Presence of Dissolved Iron and Ferrihydrite. *Environ. Sci. Technol.* **2002**, *36*, 1467–1476.

(101) Pham, A. L. T.; Doyle, F. M.; Sedlak, D. L. Kinetics and Efficiency of H2O2 Activation by Iron-Containing Minerals and Aquifer Materials. *Water Res.* **2012**, *46*, 6454–6462.

(102) Miller, C.; Valentine, R. L. Hydrogen Peroxide Decomposition and Quinoline Degradation in the Presence of Aquifer Material. *Water Res.* **1995**, *29*, 2353–2359.

(103) Valentine, R. L.; Wang, H. C. A. Iron Oxide Surface Catalyzed Oxidation of Quinoline by Hydrogen Peroxide. *J. Environ. Eng.* **1998**, *124*, 31–38.

(104) Watts, R. J.; Foget, M. K.; Kong, S. H.; Teel, A. L. Hydrogen Peroxide Decomposition in Model Subsurface Systems. *J. Hazard. Mater.* **1999**, *69*, 229–243.

(105) Pham, A. L.-T.; Doyle, F. M.; Sedlak, D. L. Inhibitory Effect of Dissolved Silica on

H_2O_2 Decomposition by Iron(III) and Manganese(IV) Oxides: Implications for H_2O_2-Based In Situ Chemical Oxidation. *Environ. Sci. Technol.* **2012**, *46*, 1055–1062.

(106) Jung, Y.; Park, J.-Y.; Ko, S.-O.; Kim, Y.-H. Stabilization of Hydrogen Peroxide Using Phthalic Acids in the Fenton and Fenton-Like Oxidation. *Chemosphere* **2013**, *90*, 812–819.

(107) Vicente, F.; Rosas, J. M.; Santos, A.; Romero, A. Improvement Soil Remediation by Using Stabilizers and Chelating Agents in a Fenton-Like Process. *Chem. Eng. J.* **2011**, *172*, 689–697.

(108) Lin, Z. R.; Zhao, L.; Dong, Y. H. Quantitative Characterization of Hydroxyl Radical Generation in a Goethite-Catalyzed Fenton-Like Reaction. *Chemosphere* **2015**, *141*, 7–12.

(109) Kertesz, M. A.; Frossard, E. Biological Cycling of Inorganic Nutrients and Metals in Soils and Their Role in Soil Biogeochemistry. In *Soil Microbiology, Ecology and Biochemistry*; Eldor, P. A., Ed.; Elsevier Inc., 2015; pp 471–503.

(110) Johnson, S. E.; Loeppert, R. H. Role of Organic Acids in Phosphate Mobilization from Iron Oxide. *Soil Sci. Soc. Am. J.* **2006**, *70*, 222.

(111) Chacon, N.; Silver, W. L.; Dubinsky, E. A.; Cusack, D. F. Iron Reduction and Soil Phosphorus Solubilization in Humid Tropical Forests Soils: The Roles of Labile Carbon Pools and an Electron Shuttle Compound. *Biogeochemistry* **2006**, *78*, 67–84.

(112) Jansson, M. Anaerobic Dissolution of Iron-Phosphorus Complexes in Sediment due to the Activity of Nitrate-Reducing Bacteria. *Microb. Ecol.* **1987**, *14*, 81–89.

(113) Hutchison, K. J.; Hesterberg, D. Dissolution of Phosphate in a Phosphorus-Enriched Ultisol as Affected by Microbial Reduction. *J. Environ. Qual.* **2004**, *33*, 1793–1802.

(114) Borggaard, O. K. Effects of Phosphate on Iron Oxide Dissolution in Ethylenediamine-N,N,N',N'-Tetraacetic Acid and Oxalate. *Clays Clay Miner.* **1991**, *39*, 32–328.

(115) Peretyazhko, T.; Sposito, G. Iron(III) Reduction and Phosphorous Solubilization in Humid Tropical Forest Soils. *Geochim. Cosmochim. Acta* **2005**, *69*, 3643–3652.

(116) Pizzigallo, M. D. R.; Ruggiero, P.; Crecchio, C.; Mascolo, G. Oxidation of Chloroanilines at Metal Oxide Surfaces. *J. Agric. Food Chem.* **1998**, *46*, 2049–2054.

(117) Singh, S.; Dosani, T.; Karakoti, A. S.; Kumar, A.; Seal, S.; Self, W. T. A Phosphate-dependent Shift in Redox State of Cerium Oxide Nanoparticles and its Effects on Catalytic Properties. *Biomaterials* **2011**, *32*, 6745–6753.

(118) Yang, X.; He, J.; Sun, Z.; Holmgren, A.; Wang, D. Effect of Phosphate on Heterogeneous Fenton Oxidation of Catechol by Nano-Fe3O4: Inhibitor or Stabilizer? *J. Environ. Sci.* **2016**, *39*, 69–76.

(119) O'Loughlin, E. J.; Gorski, C. A.; Scherer, M. M.; Boyanov, M. I.; Kemner, K. M. Effects of Oxyanions, Natural Organic Matter, and Bacterial Cell Numbers on the Bioreduction of Lepidocrocite (γ-FeOOH) and the Formation of Secondary Mineralization Products. *Environ. Sci. Technol.* **2010**, *44*, 4570–4576.

(120) Borch, T.; Masue, Y.; Kukkadapu, R. K.; Fendorf, S. Phosphate Imposed

Limitations on Biological Reduction and Alteration of Ferrihydrite. *Environ. Sci. Technol.* **2007**, *41*, 166–172.

(121) Tedersoo, L.; Bahram, M.; Toots, M.; Diedhiou, A.; Henkel, T.; Kjoller, R.; Morris, M.; Nara, K.; Nouhra, E.; Peay, K.; et al. Towards Global Patterns in the Diversity and Community Structure of Ectomycorrhizal Fungi. *Mol. Ecol.* **2012**, *21*, 4160–4170.

(122) Hiemstra, T.; Van Riemsdijk, W. H. A Surface Structural Approach to Ion Adsorption: The Charge Distribution (CD) Model. *J. Colloid Interface Sci.* **1996**, *179*, 488–508.

(123) Brunauer, S.; Emmett, P. H.; Teller, E. Adsorption of Gases in Multimolecular Layer. *J. Am. Chem. Soc.* **1938**, *60*, 309–319.

(124) *High Performance Liquid Chromatography: Fundamental Principles and Practice*; Lough, W. J., Wainer, I. W., Eds.; CRC Press, 1995.

(125) Viollier, E.; Inglett, P. W.; Hunter, K.; Roychoudhury, a N.; Van Cappellen, P. The Ferrozine Method Revisited: Fe (II)/Fe (III) Determination in Natural Waters. *Appl. Geochemistry* **2000**, *15*, 785–790.

(126) Murphy J; Riley JP. A Modified Single Solution Method for the Determination of Phosphate in Natural Waters. *Anal. Chem. ACTA* **1962**, *27*, 31–36.

(127) Gligorovski, S.; Strekowski, R.; Barbati, S.; Vione, D. Environmental Implications of Hydroxyl Radicals (OH). *Chem. Rev.* **2015**, *115*, 13051–13092.

(128) Page, S. E.; Arnold, W. A.; McNeill, K. Terephthalate as a Probe for Photochemically Generated Hydroxyl Radical. *J. Environ. Monit.* **2010**, *12*, 1658–1665.

(129) Jing, Y.; Chaplin, B. P. Mechanistic Study of the Validity of Using Hydroxyl Radical Probes To Characterize Electrochemical Advanced Oxidation Processes. *Environ. Sci. Technol.* **2017**, *51*, 2355–2365.

(130) Jaumot, J.; Gargallo, R.; De Juan, A.; Tauler, R. A Graphical User-Friendly Interface for MCR-ALS: A New Tool for Multivariate Curve Resolution in MATLAB. *Chemom. Intell. Lab. Syst.* **2005**, *76*, 101–110.

(131) Felten, J.; Hall, H.; Jaumot, J.; Tauler, R.; de Juan, A.; Gorzsás, A. Vibrational Spectroscopic Image Analysis of Biological Material Using Multivariate Curve Resolution–Alternating Least Squares (MCR-ALS). *Nat. Protoc.* **2015**, *10*, 217–240.

(132) Yuan, X.; Davis, J. A.; Nico, P. S. Iron-Mediated Oxidation of Methoxyhydroquinone Under Dark Conditions: Kinetic and Mechanistic Insights. *Environ. Sci. Technol.* **2016**, *50*, 1731–1740.

(133) Roginsky, V. A.; Pisarenko, L. M.; Bors, W.; Michel, C. The Kinetics and Thermodynamics of Quinone-Semiquinone- Hydroquinone Systems Under Physiological Conditions. *J. Chem. Soc. Trans. 2* **1999**, *2*, 871–876.

(134) Boily, J. F.; Nilsson, N.; Persson, P.; Sjöberg, S. Benzenecarboxylate Surface Complexation at the Goethite (α-FeOOH)/Water Interface: I. A Mechanistic Description of Pyromellitate Surface Complexes from the Combined Evidence of Infrared Spectroscopy, Potentiometry, Adsorption Data, and Surface Complexatio. *Langmuir* **2000**, *16*, 5719–5729.

(135) Johnson, B. B.; Sjöberg, S.; Persson, P. Surface Complexation of Mellitic Acid to Goethite: an Attenuated Total Reflection Fourier Transform Infrared Study. *Langmuir* **2004**, *20*, 823–828.

(136) Tejedor-Tejedor, M. I.; Yost, E. C.; Anderson, M. A. Characterization of Benzoic and Phenolic Complexes at the Goethite/Aqueous Solution Interface Using Cylindrical Internal Reflection Fourier Transform Infrared Spectroscopy. Part 1. Methodology. *Langmuir* **1990**, *6*, 979–987.

(137) Lindegren, M.; Persson, P. Competitive Adsorption between Phosphate and Carboxylic Acids: Quantitative Effects and Molecular Mechanisms. *Eur. J. Soil Sci.* **2009**, *60*, 982–993.

(138) Bertini, I.; Gray, H. B.; Lippard, S. J.; Valentine, J. S. Dioxygen Reactions. In *Bioinorganic Chemistry*; University Science Books, Mill Valley, CA, 1994; pp 253–313.

(139) Gorski, C. A.; Edwards, R.; Sander, M.; Hofstetter, T. B.; Stewart, S. M. Thermodynamic Characterization of Iron Oxide–Aqueous Fe 2+ Redox Couples. *Environ. Sci. Technol.* **2016**, *50*, 8538–8547.

(140) Chesworth, W.; Perez-Alberti, A.; Arnaud, E.; Morel-Seytoux, H. J.; Morel-Seytoux, H. J.; Schwertmann, U. Iron oxides. In *Encyclopedia of Soil Science*; Chesworth, W., Ed.; Springer Netherlands: Dordrecht, 2008; pp 363–369.

(141) Huynh, M. T.; Anson, C. W.; Cavell, A. C.; Stahl, S. S.; Hammes-Schiffer, S. Quinone 1 e – and 2 e – /2 H + Reduction Potentials: Identification and Analysis of Deviations from Systematic Scaling Relationships. *J. Am. Chem. Soc.* **2016**, *138*, 15903–15910.

(142) Stone, A. T.; Morgan, J. J. Reduction and Dissolution of Manganese(III) and Manganese(IV) Oxides by Organics. 1. Reaction with Hydroquinone. *Environ. Sci. Technol.* **1984**, *18*, 450–456.

(143) McBride, M. B. Adsorption and Oxidation of Phenolic Compounds by Iron and Manganese Oxides. *Soil Sci. Soc. Am. J.* **1987**, *51*, 1466–1472.

(144) Padhi, A. K.; Nanjundaswamy, K. S.; Masquelier, C.; Okada, S.; Goodenough, J. B. Effect of Structure on the Fe3 +/Fe2 + Redox Couple in Iron Phosphates. *J. Electrochem. Soc.* **1997**, *144*, 1609–1613.

(145) Alexandrov, V.; Rosso, K. M. Insights into the Mechanism of Fe(II) Adsorption and Oxidation at Fe-Clay Mineral Surfaces from First-Principles Calculations. *J. Phys. Chem. C* **2013**, *117*, 22880–22886.

(146) Alexandrov, V.; Rosso, K. M. Ab Initio Modeling of Fe(II) Adsorption and Interfacial Electron Transfer at Goethite (α-FeOOH) Surfaces. *Phys. Chem. Chem. Phys.* **2015**, *17*, 14518–14531.

(147) Anpo, M.; Che, M.; Fubini, B.; Garrone, E. Generation of Superoxide Ions at Oxide Surfaces. *Top. Catal.* **1999**, *8*, 189–198.

(148) Hiemstra, T.; Van Riemsdijk, W. H. Surface Structural Ion Adsorption Modeling of Competitive Binding of Oxyanions by Metal (Hydr)oxides. *J. Colloid Interface Sci.* **1999**, *210*, 182–193.

(149) Sundman, A.; Karlsson, T.; Laudon, H.; Persson, P. XAS Study of Iron Speciation in Soils and Waters from a Boreal Catchment. *Chem. Geol.* **2014**, *364*, 93–102.

(150) Wang, T.; Tian, Z.; Bengtson, P.; Tunlid, A.; Persson, P. Mineral-Surface-Reactive Metabolites Secreted during Fungal Decomposition Contribute to the Formation of Soil Organic Matter. *Environ. Microbiol.* **2017**, DOI: 10.1111/1462-2920.13990.

(151) Theis, T. L.; Singer, P. C. Complexation of Iron(II) by Organic Matter and Its Effect on Iron(II) Oxygenation. *Environ. Sci. Technol.* **1974**, *8* (6), 569–573.

(152) Daugherty, E. E.; Gilbert, B.; Nico, P. S.; Borch, T. Complexation and Redox Buffering of Iron(II) by Dissolved Organic Matter. *Environ. Sci. Technol.* **2017**, *51*, 11096–11104.

(153) Aeschbacher, M.; Graf, C.; Schwarzenbach, R. P.; Sander, M. Antioxidant Properties of Humic Substances. *Environ. Sci. Technol.* **2012**, *46*, 4916–4925.

(154) Walpen, N.; Schroth, M. H.; Sander, M. Quantification of Phenolic Antioxidant Moieties in Dissolved Organic Matter by Flow-Injection Analysis with Electrochemical Detection. *Environ. Sci. Technol.* **2016**, *50*, 6423–6432.

(155) Siegrist, R. L.; Crimi, M.; Simpkin, T. J. *In Situ Chemical Oxidation for Groundwater Remediation*; 2011.

(156) Khin, M. M.; Nair, A. S.; Babu, V. J.; Murugan, R.; Ramakrishna, S. A Review on Nanomaterials for Environmental Remediation. *Energy Environ. Sci.* **2012**, *5*, 8075.

(157) Sozer, N.; Kokini, J. L. Nanotechnology and its Applications in the Food Sector. *Trends Biotechnol.* **2009**, *27*, 82–89.

(158) Oberdörster, G.; Maynard, A. A.; Donaldson, K.; Castranova, V.; Fitzpatrick, J.; Ausman, K. K.; Carter, J. J.; Karn, B.; Kreyling, W. W.; Lai, D.; et al. Principles for Characterizing the Potential Human Health Effects from Exposure to Nanomaterials: Elements of a Screening Strategy. *Part. Fibre Toxicol.* **2005**, *2*, 8.

(159) Giri, S. 3 – Nanotoxicity: Aspects and Concerns in Biological Systems. In *Microbial Biodegradation and Bioremediation*; 2014; pp 55–83.

(160) Li, Y.; Zhang, Y.; Yan, B. Nanotoxicity Overview: Nano-Threat to Susceptible Populations. *Int. J. Mol. Sci.* **2014**, *15*, 3671–3697.

(161) Liu, G.; Gao, J.; Ai, H.; Chen, X. Applications and Potential Toxicity of Magnetic Iron Oxide Nanoparticles. *Small* **2013**, *9*, 1533–1545.

(162) Mahmoudi, M.; Simchi, A.; Milani, A. S.; Stroeve, P. Cell Toxicity of Superparamagnetic Iron Oxide Nanoparticles. *J. Colloid Interface Sci.* **2009**, *336*, 510–518.

(163) Fu, P. P.; Xia, Q.; Hwang, H.-M.; Ray, P. C.; Yu, H. Mechanisms of Nanotoxicity: Generation of Reactive Oxygen Species. *J. food drug Anal.* **2014**, *22*, 64–75.

(164) Khanna, P.; Ong, C.; Bay, B.; Baeg, G. Nanotoxicity: An Interplay of Oxidative Stress, Inflammation and Cell Death. *Nanomaterials* **2015**, *5*, 1163–1180.

(165) Petersen, E. J.; Nelson, B. C. Mechanisms and Measurements of Nanomaterial-Induced Oxidative Damage to DNA. *Anal. Bioanal. Chem.* **2010**, *398*, 613–650.

(166) Meng, H.; Xia, T.; George, S.; Nel, A. E. A Predictive Toxicological Paradigm for the Safety Assessment of Nanomaterials. *ACS Nano*. 2009, pp 1620–1627.

(167) Valko, M.; Leibfritz, D.; Moncol, J.; Cronin, M. T. D.; Mazur, M.; Telser, J. Free Radicals and Antioxidants in Normal Physiological Functions and Human Disease. *Int. J. Biochem. Cell Biol.* **2007**, *39*, 44–84.

(168) Kawanishi, S.; Hiraku, Y.; Murata, M.; Oikawa, S. The Role of Metals in Site-Specific DNA Damage with Reference to Carcinogenesis. *Free Radical Biology and Medicine*. 2002, pp 822–832.

(169) Niedowicz, D. M.; Daleke, D. L. The Role of Oxidative Stress in Diabetic Complications. *Cell Biochem. Biophys.* **2005**, *43*, 289–330.

(170) Reuter, S.; Gupta, S. C.; Chaturvedi, M. M.; Aggarwal, B. B. Oxidative Stress, Inflammation, and Cancer: How are They Linked? *Free Radical Biology and Medicine*. 2010, pp 1603–1616.

(171) Perry, G.; Cash, A. D.; Smith, M. A. Alzheimer Disease and Oxidative Stress. *J. Biomed. Biotechnol.* **2002**, *2*, 120–123.

(172) Trachootham, D.; Alexandre, J.; Huang, P. Targeting Cancer Cells by ROS-Mediated Mechanisms: a Radical Therapeutic Approach? *Nat. Rev. Drug Discov.* **2009**, *8*, 579–591.

(173) Wang, D.; Zhao, L.; Ma, H.; Zhang, H.; Guo, L.-H. Quantitative Analysis of Reactive Oxygen Species Photogenerated on Metal Oxide Nanoparticles and Their Bacteria Toxicity: The Role of Superoxide Radicals. *Environ. Sci. Technol.* **2017**, *51*, 10137–10145.

Acknowledgements

This PhD project was supported by grants from the Swedish Research Council (VR, Grant no. 621-2012-3890), the Knut and Alice Wallenberg Foundation (2013.0073), the Crafoord Foundation and the Faculty of Science, Lund University. Part of experimental work was conducted at the Vibrational Spectroscopy Core Facility, Umeå University. The platform manager, Dr. Andras Gorzsas, is gratefully acknowledged for his support.

These have been a few amazing years and this would not have been possible (and half as much fun) without a help of few people:

My main supervisor **Per Persson**, I could not have asked for a better supervisor. Thank you for giving me this opportunity, being supportive and patient. You have taught me so much over these years, when I could not explain or understand something, you always had answers. Your endless knowledge and enthusiasm never stopped to amaze me. Thank you for encourage and inspiration to always get things done better.

My co-adviser **Anders Tunlid,** thank you for scientific discussions, explanations and feedbacks. It was a pleasure to work and learn new things from you.

Gry, thanks for always making work fun. You were the best support system and excellent companion during the long days in the dark and trying to get through the glove bag experiments.

Cesar, you were the best office mate ever. Thank you for all the scientific and not so scientific discussions and, of course, for improving my Spanish. Gracias!

Michiel and Dimitri, thank you for your countless fungi consultations and for adding all the missing "the". You were an amazing help.

Rest of the MICCS group members, **Luigi, Tao, Tian, Johan, Shakil, Firoz, Tomas B., Carl, Tomas J.**, this was a great experience working in such a diverse research group. I have learnt so much from you all.

Microbial Ecology group members, **Margarida, Kristin R. Kristin A., Saeed, Johannes, Edith, Per B., Håkan, Eva B., Eva F., Juan Pablo, Mikaela, Lettice, Erland, Carlos, Ainara, Anna,** for all the fun at lunches and countless "fikas".

Sofia, you were a great support and fun when I needed, especially in the last few weeks.

To all PhD students in Environmental Science program, your friendship made this journey more exciting.

To the rest of CEC and MEMEG colleagues and everyone else who helped me even with the smallest questions.

All the amazing people that I met at the beginning of my PhD journey in Umeå. It has been a pleasure knowing you all. **Diana and Merve** you have been amazing friends all these years. We started the PhD journey together and we are finishing at the same time. Cannot wait to see what great adventures the future will bring to us.

My family and friends. Paldies vecākiem, bez jūsu atbalsta un pacietības daudz kas nebūtu bijis iespējams. Agnese, Agnija, Inese un Santa, ko gan es bez jums iesāktu!

Papers I-V

I. Krumina, L., Lyngsie, G., Tunlid, A., Persson, P. Oxidation of a dimethoxyhydroquinone by ferrihydrite and goethite nanoparticles: Iron reduction versus surface catalysis. *Environmental Science & Technology,* 51, 9053-9061, 2017.

II. Lyngsie, G., Krumina, L., Tunlid, A., Persson, P. Generation of hydroxyl radicals from reactions between a dimethoxyhydroquinone and iron oxide nanoparticles. *Submitted to Environmental Science: Nano.*

III. Krumina, L., Persson, P. Mutual influence of hydroquinone oxidation and phosphate adsorption at iron oxide surfaces. *Manuscript.*

IV. Krumina, L., Kenney, J. P.L., Loring, J. S., Persson, P. Desorption mechanisms of phosphate from ferrihydrite and goethite surfaces. *Chemical Geology*, 427, 54-64, 2016.

V. Krumina, L., Ob De Beeck, M., Tunlid, A., Persson, P. Fungal decomposition of dissolved organic matter (DOM): Consequences for reductive dissolution of iron oxides and hydroxyl radical production. *Manuscript.*

Printed by Media-Tryck, Lund 2017 NORDIC ECOLABEL. 3041 0903

Faculty of Science
Centre for Environmental and Climate Research
Department of Biology
ISBN 978-91-7753-503-4 (print)
ISBN 978-91-7753-504-1 (pdf)